

AD-A014 738

THREE-DIMENSIONAL SHOCK WAVE-TURBULENT
BOUNDARY LAYER INTERACTIONS AT MACH 6

C. Herbert Law

Aerospace Research Laboratories
Wright-Patterson Air Force Base, Ohio

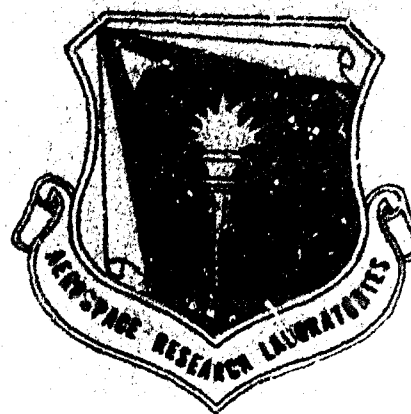
June 1975

DISTRIBUTED BY:

NTIS

National Technical Information Service
U. S. DEPARTMENT OF COMMERCE

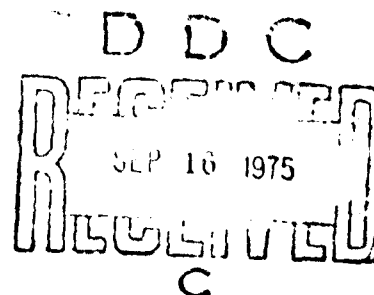
A014738



THREE-DIMENSIONAL SHOCK WAVE-TURBULENT BOUNDARY LAYER INTERACTIONS AT MACH 6

THEORETICAL AERODYNAMICS RESEARCH LABORATORY (ARI)

JUNE 1975



INTERIM REPORT JULY 1974 - OCTOBER 1974

Approved for public release; distribution unlimited

THEORETICAL AERODYNAMICS RESEARCH LABORATORY/LH
AEROSPACE RESEARCH LABORATORIES
Building 450 - Area B
Wright-Patterson Air Force Base, Ohio 45433

NATIONAL TECHNICAL
INFORMATION SERVICE

AIR FORCE SYSTEMS COMMAND
United States Air Force



**Best
Available
Copy**

NOTICES

When Government drawings, specifications, or other data are used for any purpose other than in connection with a definitely related Government procurement operation, the United States Government thereby incurs no responsibility nor any obligation whatsoever; and the fact that the Government may have formulated, furnished, or in any way supplied the said drawings, specifications, or other data, is not to be regarded by implication or otherwise as in any manner licensing the holder or any other person or corporation, or conveying any rights or permission to manufacture, use, or sell any patented invention that may in any way be related thereto.

Organizations or individuals receiving reports via Aerospace Research Laboratories automatic mailing lists should refer to the ARL number of the report received when corresponding about change of address or cancellation. Such changes should be directed to the specific laboratory originating the report. Do not return this copy; retain or destroy.

Reports are not stocked by the Aerospace Research Laboratories. Copies may be obtained from:

National Technical Information Service
Clearinghouse
Springfield, VA 22161

This technical report has been reviewed and is approved for publication.

FOR THE COMMANDER:

Elizabeth Day
ELIZABETH DAY
Technical Documents
and STINFO Office

ADDITION TO	
NTIS	Write Section <input checked="" type="checkbox"/>
D-15	Edit Section <input type="checkbox"/>
UNCLASSIFIED	<input type="checkbox"/>
JUSTIFICATION	
BY	
DISTRIBUTION/AVAILABILITY STATE	
Natl.	Avail. and/or Special
A	

This report has been reviewed and cleared for open publication and public release by the appropriate Office of Information in accordance with AFR 190-12 and DODD 5230.0. There is no objection to unlimited distribution of this report to the public at large, or by DDC to the National Technical Information Service.

Unclassified

SECURITY CLASSIFICATION OF THIS PAGE (When Data Entered)

REPORT DOCUMENTATION PAGE		READ INSTRUCTIONS BEFORE COMPLETING FORM
1. REPORT NUMBER ARL 75-0191	2. GOVT ACCESSION NO.	3. RECIPIENT'S CATALOG NUMBER AD-A014 738
4. TITLE (and Subtitle) THREE-DIMENSIONAL SHOCK WAVE-TURBULENT BOUNDARY LAYER INTERACTIONS AT MACH 6	5. TYPE OF REPORT & PERIOD COVERED Technical - Final July 1974 - October 1974	
7. AUTHOR(s) C. Herbert Law	6. PERFORMING ORG. REPORT NUMBER	
9. PERFORMING ORGANIZATION NAME AND ADDRESS Aerospace Research Laboratories (AFSC) Theoretical Aerodynamics Research Laboratory (Lab.) Wright-Patterson AFB, OH 45433	8. CONTRACT OR GRANT NUMBER(s)	
11. CONTROLLING OFFICE NAME AND ADDRESS Aerospace Research Laboratories (ARL) Bldg. 450, Area B Wright-Patterson AFB, OH 45433	10. PROGRAM ELEMENT, PROJECT, TASK AREA & WORK UNIT NUMBERS Project 7064-06-11 61102F	
14. MONITORING AGENCY NAME & ADDRESS (if different from Controlling Office)	12. REPORT DATE June 1975	
	13. NUMBER OF PAGES 49	
	15. SECURITY CLASS. (of this report) Unclassified	
	15a. DECLASSIFICATION/DOWNGRADING SCHEDULE	
16. DISTRIBUTION STATEMENT (of this Report)		
<div style="border: 1px solid black; padding: 5px; text-align: center;"> DISTRIBUTION STATEMENT A Approved for public release; Distribution Unlimited </div>		
17. DISTRIBUTION STATEMENT (of the abstract entered in Block 20, if different from Report)		
Approved for public release; distribution unlimited.		
18. SUPPLEMENTARY NOTES		
19. KEY WORDS (Continue on reverse side if necessary and identify by block number)		
Boundary layer Separation Hypersonic Shock Three-dimensional Turbulent		
20. ABSTRACT (Continue on reverse side if necessary and identify by block number)		
<p>Experimental results of an investigation of the three-dimensional interaction between a skewed shock wave and a turbulent boundary layer are presented. Surface pressure and heat transfer distributions and oil flow photographs were obtained at a freestream Mach number of 5.85 and two Reynolds numbers of ten and twenty million per foot. The model configuration consisted of a shock generator mounted perpendicularly to a flat plate. The shock generator leading edge was sharp and nonswept and intersected the flat plate surface about 8.5</p>		

DD FORM 1 JAN 73 1473

EDITION OF 1 NOV 65 IS OBSOLETE

Unclassified

SECURITY CLASSIFICATION OF THIS PAGE (When Data Entered)

AIR FORCE - 7-2-75 - 200

UNCLASSIFIED

SECURITY CLASSIFICATION OF THIS PAGE(When Data Entered)

inches downstream of the flat plate leading edge. The shock generator surface was 7.55 inches long and 3 inches high and its angle to the freestream flow was adjusted from 4 to 20 degrees. The generated shock waves were of sufficient strength to produce turbulent boundary layer separation on the flat plate surface. The extent of separation increased with increasing shock generator angle. The peak heating value near reattachment increased with increasing shock generator angle for fixed Reynolds number, and decreased with increasing Reynolds number for fixed shock generator angle. The locations of peak pressure and heat transfer were coincident and roughly equal to 40 to 45 per cent of the distance to the shock location. Peak heating values or seven times the local undisturbed values were measured.

102

Unclassified

SECURITY CLASSIFICATION OF THIS PAGE(When Data Entered)

PREFACE

Dr. C. Herbert Law of the Theoretical Aerodynamics Research Laboratory, Aerospace Research Laboratories, Air Force Systems Command, performed the work presented in this report under Project 7064, entitled "High Speed Aerodynamics."

The tests were conducted in the Aerospace Research Laboratories' Mach 6 high Reynolds number wind tunnel between July 1974 and October 1974. This report presents the results of an investigation of turbulent boundary layer separation produced by a skewed shock wave.

TABLE OF CONTENTS

SECTION		PAGE
I	INTRODUCTION	1
II	EXPERIMENTAL PROCEDURE	4
	1. Wind Tunnel Description.	4
	2. Model Design	4
	3. Instrumentation.	5
III	DISCUSSION OF RESULTS.	7
IV	SUMMARY AND CONCLUSIONS.	10
	REFERENCES	39
	LIST OF SYMBOLS.	40

LIST OF ILLUSTRATIONS

FIGURE		PAGE
1	Model Configuration and Coordinate System.	11
2	Flowfield Configuration of Shock Wave- Boundary Layer Interaction Where Skewed Shock Wave is of Sufficient Strength to Cause Separation	12
3	Surface Streamline Pattern for Separated Skewed Shock Wave-Boundary Layer Interaction	13
4	Model Configuration and Nomenclature	14
5	Model and Wind Tunnel Configurations for Injected and Ejected Positions	15
6	Measured Flat Plate Undisturbed Heat Transfer Distribution.	16
7	Mach Number Distribution through Boundary Layer on Flat Plate at Station 5	17
8	Boundary Layer Thickness Calculated from Finite Difference Scheme	18
9a	Surface Heat Transfer Distributions for $Re = 1.0 \times 10^7$ and $3.0 \times 10^7 \text{ ft}^{-1}$ and $\delta_{SG} = 4^\circ$	19
9b	Surface Heat Transfer Distributions for $Re = 1.0 \times 10^7$ and $3.0 \times 10^7 \text{ ft}^{-1}$ and $\delta_{SG} = 5^\circ$	20
9c	Surface Pressure and Heat Transfer Distributions for $Re = 1.0 \times 10^7 \text{ ft}^{-1}$ and $\delta_{SG} = 6^\circ$	21
9d	Surface Pressure and Heat Transfer Distributions for $Re = 3.0 \times 10^7 \text{ ft}^{-1}$ and $\delta_{SG} = 6^\circ$	22
9e	Surface Pressure and Heat Transfer Distributions for $Re = 1.0 \times 10^7 \text{ ft}^{-1}$ and $\delta_{SG} = 8^\circ$	23
9f	Surface Pressure and Heat Transfer Distributions for $Re = 3.0 \times 10^7 \text{ ft}^{-1}$ and $\delta_{SG} = 8^\circ$	24

9g	Surface Pressure and Heat Transfer Distributions for $Re = 1.0 \times 10^7 \text{ ft}^{-1}$ and $\delta_{SG} = 10^\circ$	25
9h	Surface Pressure and Heat Transfer Distributions for $Re = 3.0 \times 10^7 \text{ ft}^{-1}$ and $\delta_{SG} = 10^\circ$	26
9i	Surface Pressure and Heat Transfer Distributions for $Re = 1.0 \times 10^7 \text{ ft}^{-1}$ and $\delta_{SG} = 12^\circ$	27
9j	Surface Pressure and Heat Transfer Distributions for $Re = 3.0 \times 10^7 \text{ ft}^{-1}$ and $\delta_{SG} = 12^\circ$	28
9k	Surface Pressure and Heat Transfer Distributions for $Re = 1.0 \times 10^7 \text{ ft}^{-1}$ and $\delta_{SG} = 16^\circ$	29
9l	Surface Pressure and Heat Transfer Distributions for $Re = 3.0 \times 10^7 \text{ ft}^{-1}$ and $\delta_{SG} = 16^\circ$	30
9m	Surface Pressure and Heat Transfer Distributions for $Re = 1.0 \times 10^7 \text{ ft}^{-1}$ and $\delta_{SG} = 20^\circ$	31
9n	Surface Pressure and Heat Transfer Distributions for $Re = 3.0 \times 10^7 \text{ ft}^{-1}$ and $\delta_{SG} = 20^\circ$	32
10a	Sketch of Oil Flow Photograph for $Re = 1.0 \times 10^7 \text{ ft}^{-1}$ and $\delta_{SG} = 8^\circ$	33
10b	Sketch of Oil Flow Photograph for $Re = 1.0 \times 10^7 \text{ ft}^{-1}$ and $\delta_{SG} = 10^\circ$	34
10c	Sketch of Oil Flow Photograph for $Re = 1.0 \times 10^7 \text{ ft}^{-1}$ and $\delta_{SG} = 12^\circ$	35
10d	Sketch of Oil Flow Photograph for $Re = 1.0 \times 10^7 \text{ ft}^{-1}$ and $\delta_{SG} = 16^\circ$	36
10e	Sketch of Oil Flow Photograph for $Re = 1.0 \times 10^7 \text{ ft}^{-1}$ and $\delta_{SG} = 20^\circ$	37
11	Lateral Distance to Shock Generator Surface, Shock, Reattachment Line and Separation Line Versus Shock Generator Angle.	38

SECTION I

INTRODUCTION

Interactions between shock waves and boundary layers have been investigated because they can produce local aerodynamic heating rates several times larger than anticipated. These interactions can be present in the wing/body and fin/body junctions of high speed vehicles, and are typically three-dimensional. One of the more common configurations that cause shock wave induced boundary layer separation is the axial corner, where the shock wave generated by one compression surface impinges on the boundary layer of the second surface. The imposed adverse pressure gradient on the boundary layer flow can produce separation which, in the three-dimensional case, will scavenge off the low energy flow of the boundary layer. The reattaching flow consists of high energy air which causes elevated heating rates near the axial corner.

This report presents the results of an investigation of turbulent boundary layer separation produced by a skewed shock wave. The shock wave was produced by a shock generator whose nonswept leading edge was perpendicular to the uniform freestream flow. The test boundary layer was produced on a flat plate whose surface was aligned with the freestream flow. The model configuration is shown in Fig. 1.

In an elementary sense, the skewed shock wave interaction is similar to the two-dimensional planar shock wave interaction if viewed in a cross section plane perpendicular to the skewed shock. In this plane the skewed shock appears normal to the surface, and a crossflow is present and perpendicular to the plane. Basically the inviscid flow field is conical

in nature, which is to say the flow structure grows linearly from the shock generator leading edge. The viscous interaction region is generally not conical, and varies nonlinearly in the axial direction because the boundary layer characteristics are changing nonlinearly. However, for high Reynolds numbers and turbulent flow in the interaction region, the boundary layer is thin and the interaction configuration is dominated by the inviscid flow field. Under these conditions, the flow field can be assumed nearly conical downstream of the immediate vicinity of the shock generator leading edge-flat plate junction. For large shock generator angles and correspondingly large regions of separation, this assumption is not valid. In general, at any given axial station, the flow field will resemble that shown in Fig. 2.

The objectives of this investigation were to identify the surface characteristics of the skewed shock wave-turbulent boundary layer interaction in the corner region of the flat plate-fin configuration. The complicated structure of the inviscid flow field was not investigated or analyzed, and, in general, for this configuration would be relatively independent of the viscous interaction for small regions of separation. Whatever the inviscid structure of the corner region, for sufficiently large shock generator angles the imposed adverse pressure gradient is sufficient to cause separation. The low energy flow in the boundary layer is scavenged off by the crossflow vortex, and only the outer flow in the boundary layer has sufficient energy to negotiate the adverse pressure gradient. The resulting surface streamline pattern is shown in Fig. 3.

In this investigation, surface oil flow patterns and lateral distributions of surface pressure and heat transfer at five axial stations

were obtained for two freestream unit Reynolds numbers of 1.0 and 3.0×10^7 per foot at a Mach number of 5.90. Shock generator angles of 4 to 20 degrees were investigated.

SECTION II

EXPERIMENTAL PROCEDURE

1. WIND TUNNEL DESCRIPTION

The tests were conducted in the Aerospace Research Laboratories' Mach 6 high Reynolds number wind tunnel. This facility is a blowdown wind tunnel which operates at stagnation pressures from 700 to 2100 psia and a stagnation temperature of 1100°R (550°F). The test region is an open jet approximately 18 inches long with a core diameter of 10 inches. a complete description of the facility is given in Ref. 1.

2. MODEL DESIGN

The model consisted of a sharp leading edge flat plate with a 10-inch span and a 16-inch chord. The shock generator consisted of a sharp leading edge fin with a chord of 7.55 inches and a height of 3 inches. The shock generator was mounted to the flat plate with its surface and leading edge perpendicular to the flat plate surface. The leading edge of the shock generator was approximately 8.5 inches downstream of the flat plate leading edge. The shock generator angle could be varied from 0 to 20 degrees (compression), and the surface could be moved laterally across the flat plate to shift the interaction region with respect to the instrumentation on the flat plate. The shock generator was not instrumented. The model configuration is shown in Fig. 4.

The model was mounted in the wind tunnel on a rigid support strut. The flat plate surface was aligned parallel to the freestream flow. Prior to wind tunnel starting, the model was ejected from the test section into the test cabin. After wind tunnel starting and stabilization (5-10 seconds),

the model was injected into the test core (~ 2 seconds) and appropriate data were then recorded. After run times from 10 to 60 seconds, the model was ejected from the test section prior to wind tunnel shutdown. The model/wind tunnel configuration is shown in Fig. 5.

3. INSTRUMENTATION

The flat plate model had three 10 x 10 inch square inserts to obtain measurements of surface pressure and temperature and oil flow visualizations. One insert was instrumented with 60 iron-constantan thermocouples spot welded on the back side of the insert at the locations indicated in Fig. 4. The region along each thermocouple row was milled out to a nominal 0.040-inch thickness to provide a thin-skin surface at least 0.5 inch in all directions from each thermocouple. Each thermocouple output was connected to a separate channel of a Research, Inc., Model 812-11 Universal Signal Conditioner and Reference Junction Compensator operating at a thermostatically controlled reference temperature of 150°F.

The pressure distribution model insert was instrumented with 55 pressure orifices at the locations indicated in Fig. 4. The pressure orifices were connected to multiple Scanivalve Model 48CBM rotating valves with built-in variable reluctance transducers.

The oil flow visualization model insert consisted of a blank plate with its surface painted flat-black and reference scribed with 0.5-inch-square grids. The oil flow visualization was achieved with a mixture of silicone oil, titanium dioxide, oleic acid and "STP" oil. The best results were obtained by spreading thin lines of oil on the model surface along the lateral grid lines. Short runs of 10 to 15 seconds were required to

achieve desirable results. Measurements and photographs of the oil flow pattern were made after wind tunnel shutdown.

The outputs from the signal conditioners were recorded on-line in analogue form on X-Y recorders. The data were also digitized and recorded on magnetic tape by an Adage Model 200 Ambilog computer for later reduction and analysis on a CDC 6600 computer. A complete description of the data reduction procedures to obtain heat transfer data from the thermocouple outputs is contained in Ref. 2.

SECTION III

DISCUSSION OF RESULTS

Surface pressure and heat transfer data and oil flow photographs were obtained for two freestream unit Reynolds numbers of 1.0 and 3.0×10^7 per foot and for eight shock generator angles between 4 and 20 degrees. Pressure and temperature data were obtained at 0.125-inch increments along each axial station by moving the shock generator with respect to the flat plate instrumentation. The local undisturbed reference values of static pressure and heat transfer were obtained without the shock generator. The reference static pressure was nearly constant over the entire flat plate surface and corresponded to a freestream Mach number of 5.85. The reference distributions of heat transfer on the flat plate centerline are shown in Fig. 6. All heating values were measured with an initial uniform flat plate wall temperature near ambient, or approximately 50% of the adiabatic wall temperature.

A total pressure survey through the undisturbed flat plate turbulent boundary layer at station 5 was made with a pitot tube rake. The resulting Mach number distribution for one Reynolds number is shown in Fig. 7 and compared with theoretical calculation results obtained by an implicit finite difference numerical scheme with intermittency correction. The calculated undisturbed boundary layer thicknesses along the flat plate for both Reynolds numbers investigated are shown in Fig. 8.

The lateral distributions of static pressure and heat transfer at stations 4 and 5 are presented in Fig. 9. The pressures and heat transfer values have been nondimensionalized by the local undisturbed reference values. The distributions have been presented as a percentage of the local

lateral distance between the shock generator surface and the shock wave. This coordinate allows for more direct comparison between distributions obtained along different axial stations. If the flow field were truly conical, the distribution along station 4 should be identical to that along station 5 in the present coordinate system. Of the distributions presented, only the static pressure distributions for a shock generator angle of 20° show noticeable departure from conical flow between stations 4 and 5.

The present coordinate system also allows approximate comparisons to be made between distributions for different shock generator angles. At a given station, the lateral distance between the shock generator surface and the shock wave changes very little for shock generator angles between 3° and 16° ($\bar{Y}_s = 0.95$ at $\delta_{SG} = 3^\circ$ and 16° , $\bar{Y}_s = 0.87$ at $\delta_{SG} = 10^\circ$ for an axial distance of 6 inches downstream of the shock generator leading edge).

Sketches of the oil flow photographs are shown in Fig. 10 for shock generator angles of 8° through 20° and a Reynolds number of $1 \times 10^7 \text{ ft}^{-1}$. The locations of separation and reattachment obtained from the oil flow photographs are indicated on the pressure and heat transfer distributions presented in Fig. 9. The separation line is represented by converging surface streamlines and the reattachment line is represented by diverging streamlines. In general, the separation and reattachment lines were quite linear, except near the shock generator leading edge. The oil flow patterns did not appear to be sensitive to Reynolds number.

The locations of separation and reattachment are also shown in Fig. 11 as they varied with shock generator angle. While the distance between the surface and the separation line increased dramatically with increasing shock generator angle, the distances between the surface and the reattachment line

and the shock wave were nearly constant. Near the incipient separation angle, approximately between 2 and 3°, one would expect the location of separation and reattachment to be nearly coincident with the shock wave location.

In general, the locations of peak surface pressure and heat transfer were coincident, and roughly equal to 40 to 45% of the distance to the shock location. The peak heating value increased with shock generator angles and peak pressure for fixed freestream Reynolds number, and decreased with increasing Reynolds number for fixed shock generator angle (and fixed peak pressure). No attempt was made to correlate the peak heat values with peak pressure for two reasons. First, the small density of data points did not give accuracy in choosing the correct peak value. Second, as was pointed out in Ref. 2, the heating data presented here were not corrected for conduction losses. Estimates showed that these losses were significant, at least in the peak heating region, and that they could amount to 15 to 25% of the peak heating value.

Only the gross features of the skewed shock wave-turbulent boundary layer interaction have been discussed here. No attempts were made to define the fine, detailed structure of the interaction or the inviscid flow field, although these investigations will continue. Of particular importance is the interior structure of the separated region for large shock generator angles. The "dips" in the surface pressure distributions, the interior small peaks in the heat transfer distributions, and the secondary flow in the oil flow patterns indicate the possibility of the existence of secondary vortices for large regions of separation. These and other problems will be investigated in more detail in the future.

SECTION IV

SUMMARY AND CONCLUSIONS

The results of an experimental investigation of the three-dimensional interaction between a skewed shock wave and a turbulent boundary layer have been presented. The tests were conducted at a freestream Mach number of 5.85 and two Reynolds numbers of 1.0×10^7 and 3.0×10^7 per foot. Surface pressure and heat transfer distributions and oil flow photographs were obtained to define the scale of the interactions for shock generator angles between 4° and 20° . The conclusions drawn from this investigation are:

- 1) The distance between the shock generator surface and the separation line increased with increasing shock generator angle while the distance between the surface and the shock wave and reattachment remained nearly constant.
- 2) The locations of peak surface pressure and heat transfer were coincident and roughly equal to 40 to 45% of the distance to the shock location.
- 3) The peak heating value increased with shock generator angle and peak pressure for fixed freestream Reynolds number, and decreased with increasing Reynolds number for fixed shock generator angle.
- 4) The viscous interaction was nearly conical except in the immediate vicinity of the shock generator leading edge and for very large shock generator angles, greater than 16° .

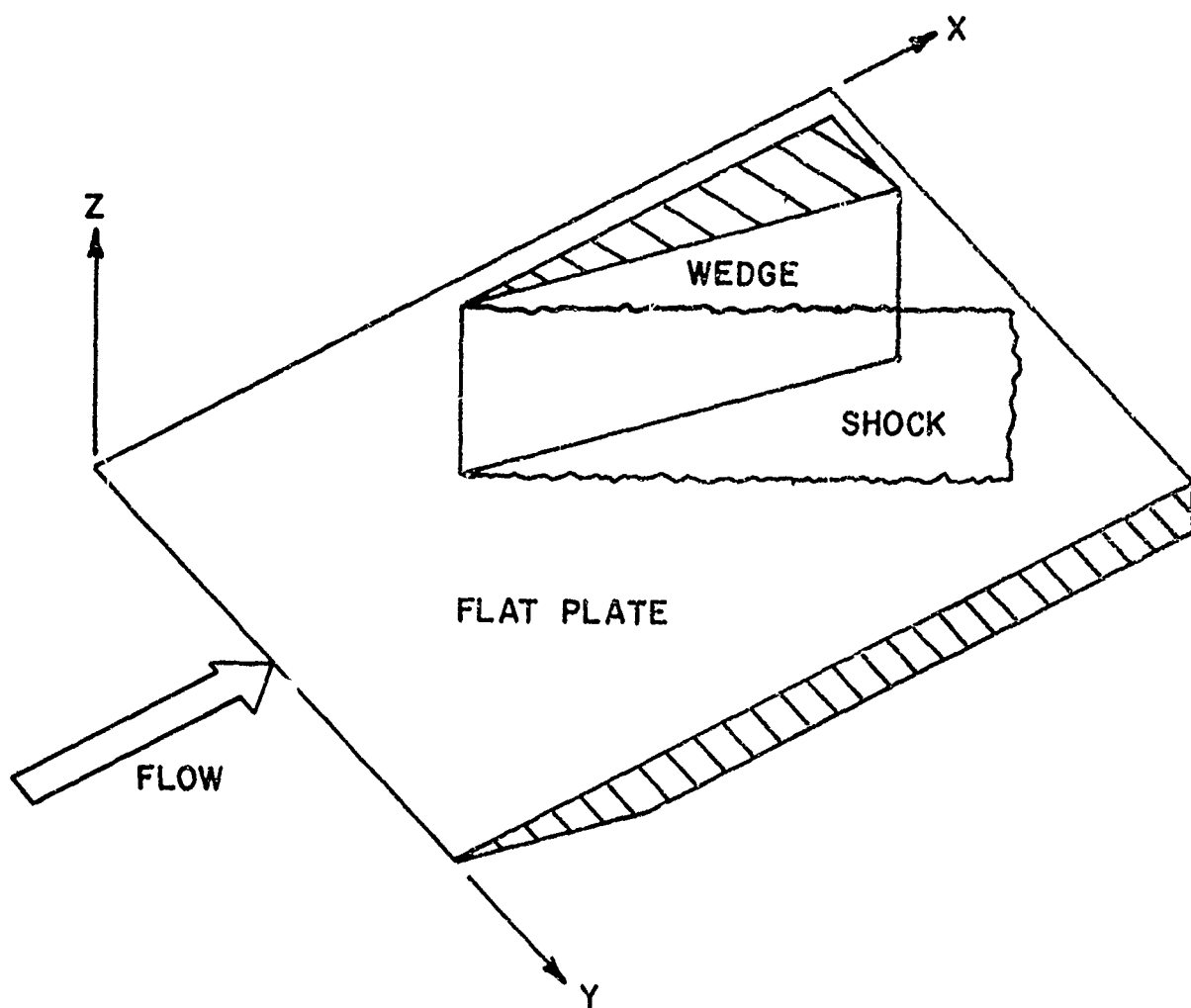


Figure 1. Model Configuration and Coordinate System

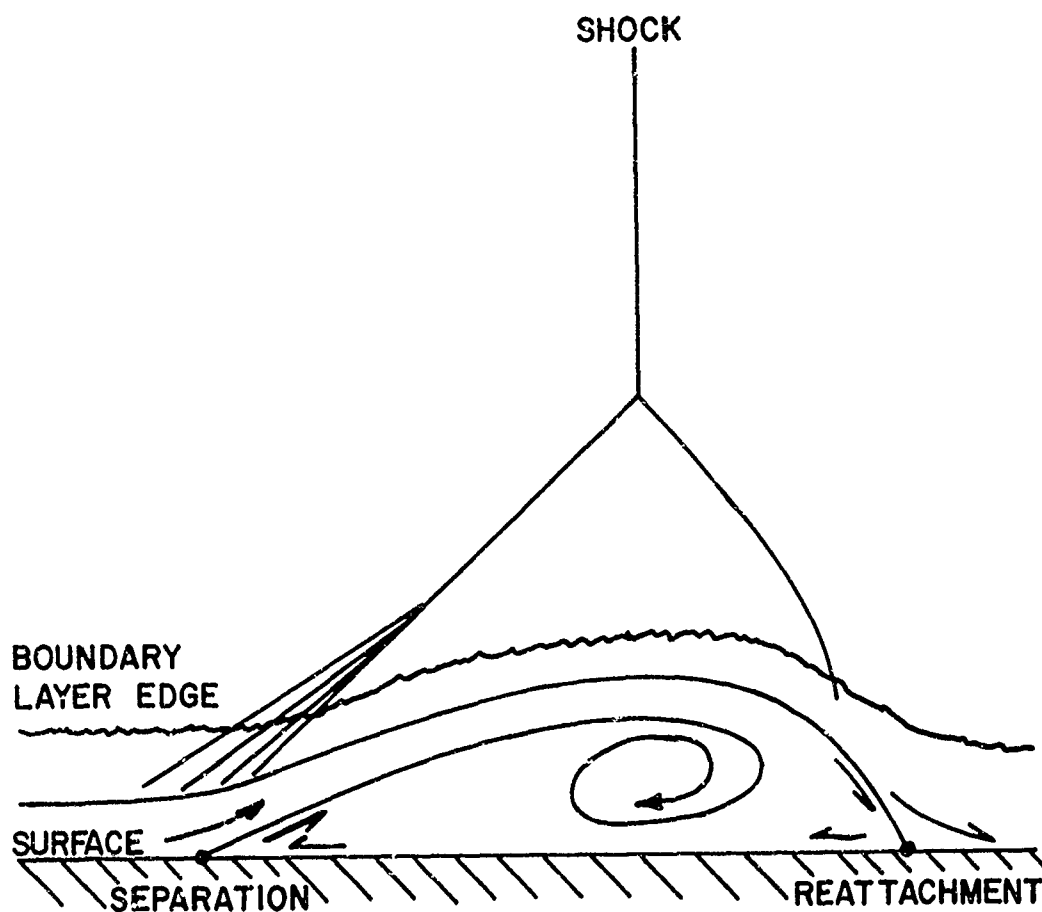


Figure 2. Flowfield Configuration of Shock Wave-Boundary Layer Interaction Where Skewed Shock Wave is of Sufficient Strength to Cause Separation

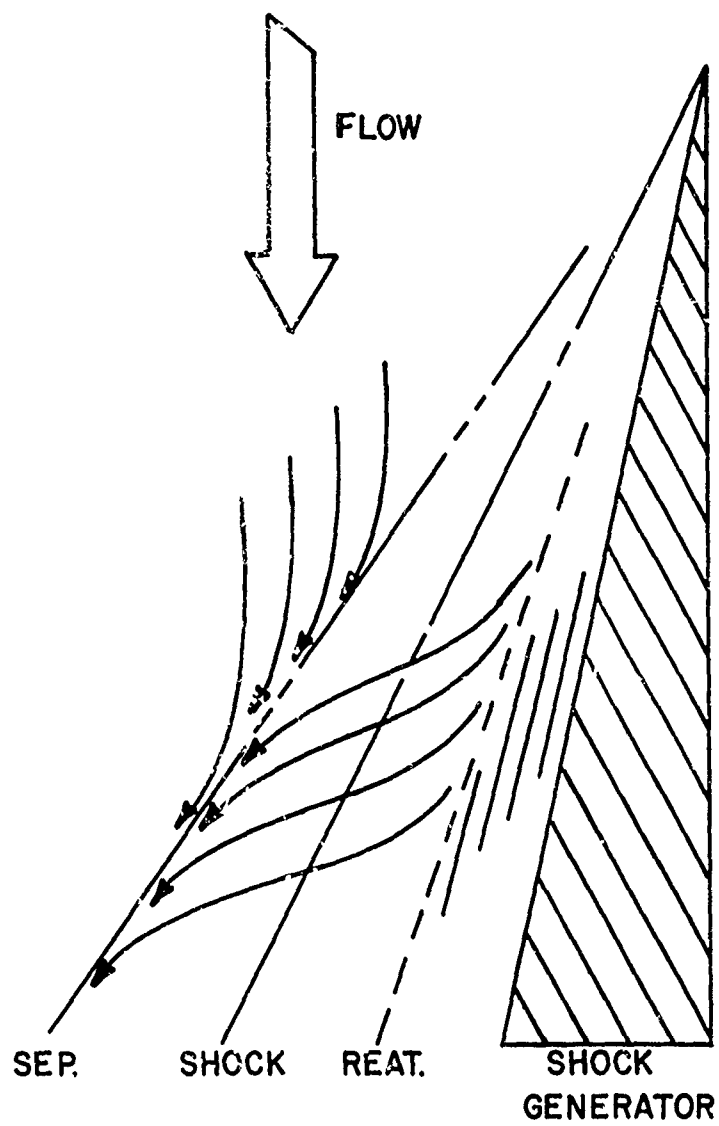


Figure 3. Surface Streamline Pattern for Separated Skewed Shock Wave-Boundary Layer Interaction

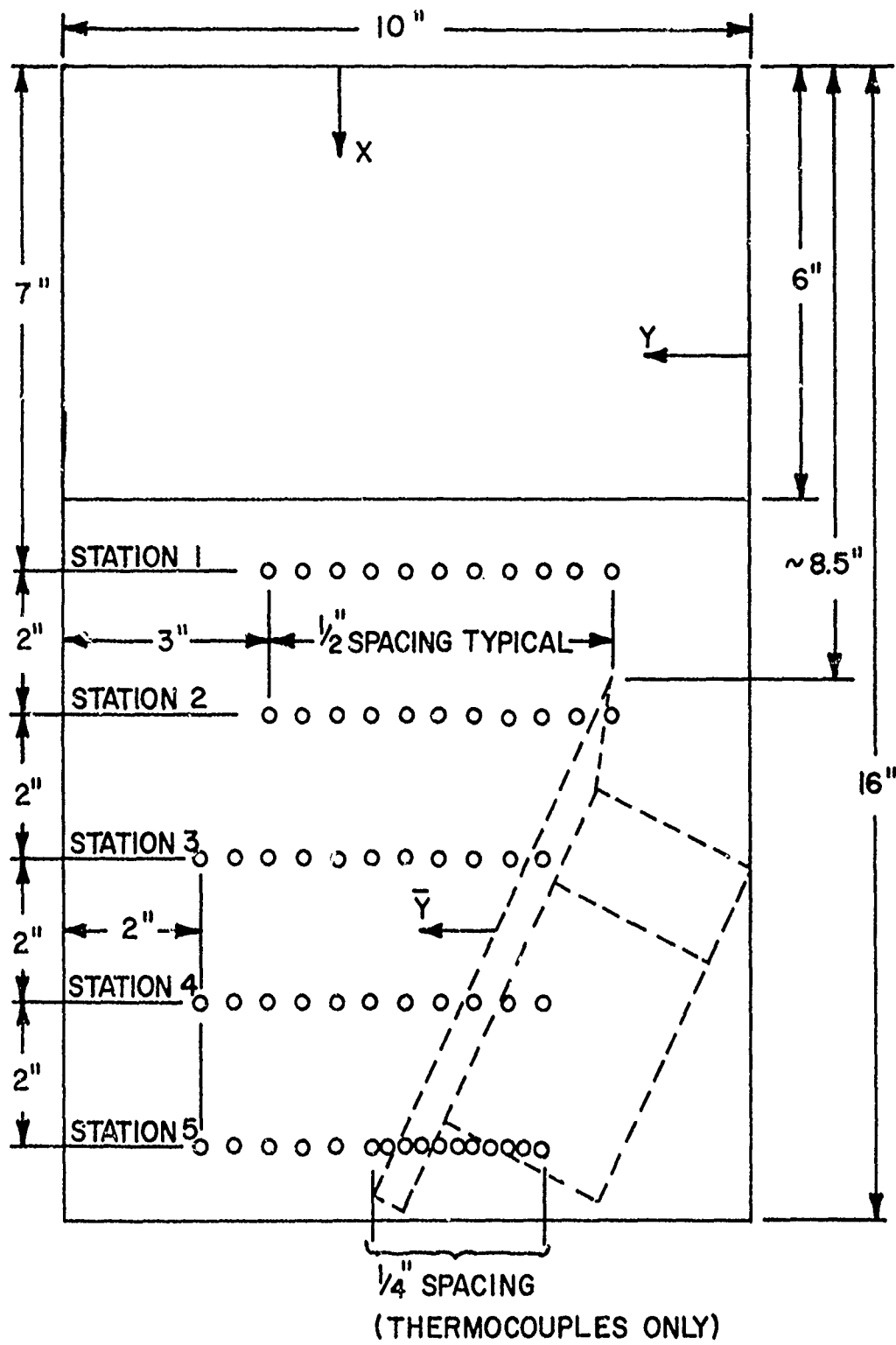


Figure 4. Model Configuration and Nomenclature

DIFFUSER
COLLECTOR

NOZZLE

INJECTED

EJECTED

ϕ

Figure 5. Model and Wind Tunnel Configurations for Injected and Ejected Positions

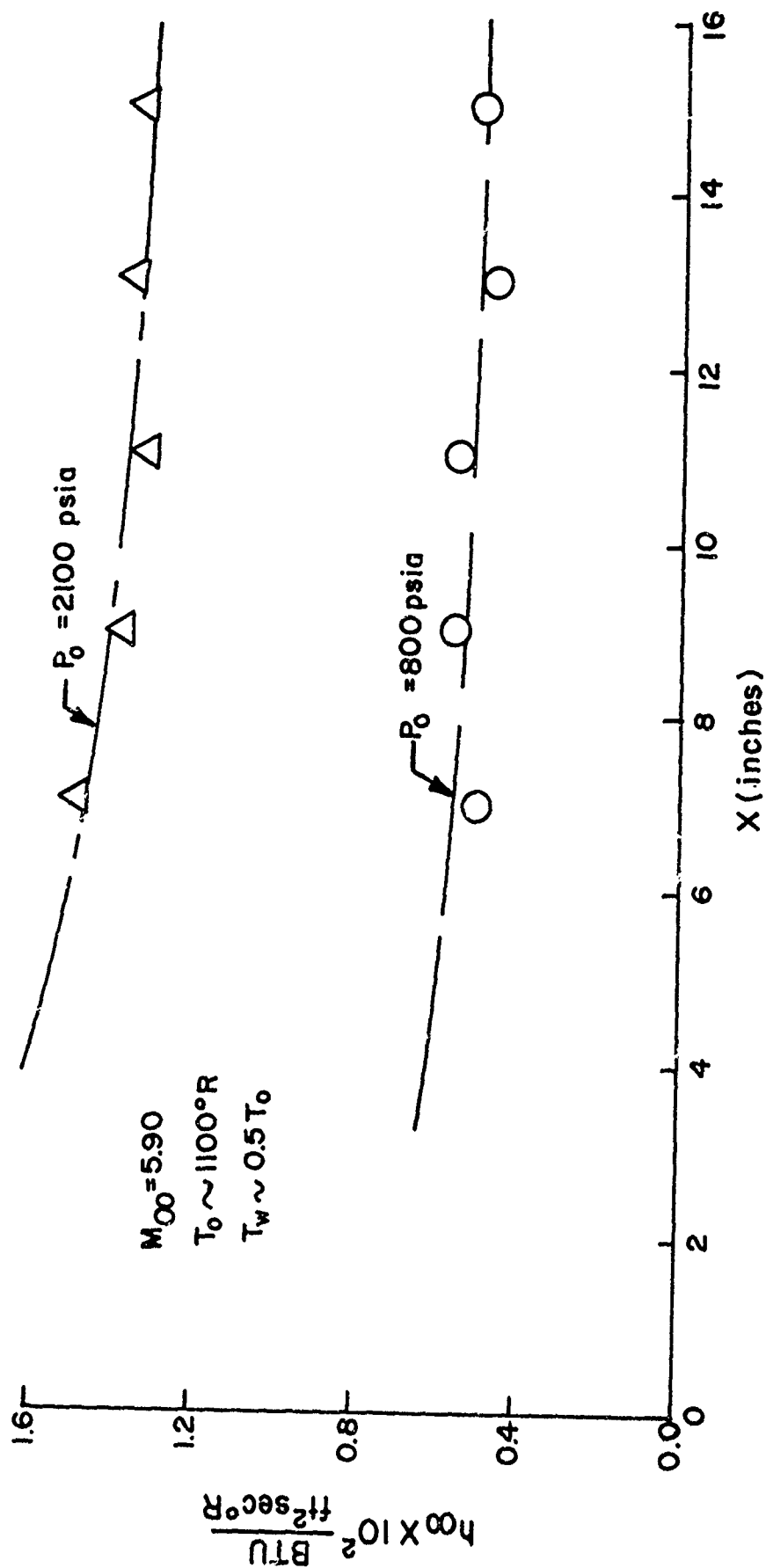


Figure 6. Measured Flat Plate Undisturbed Heat Transfer Distribution

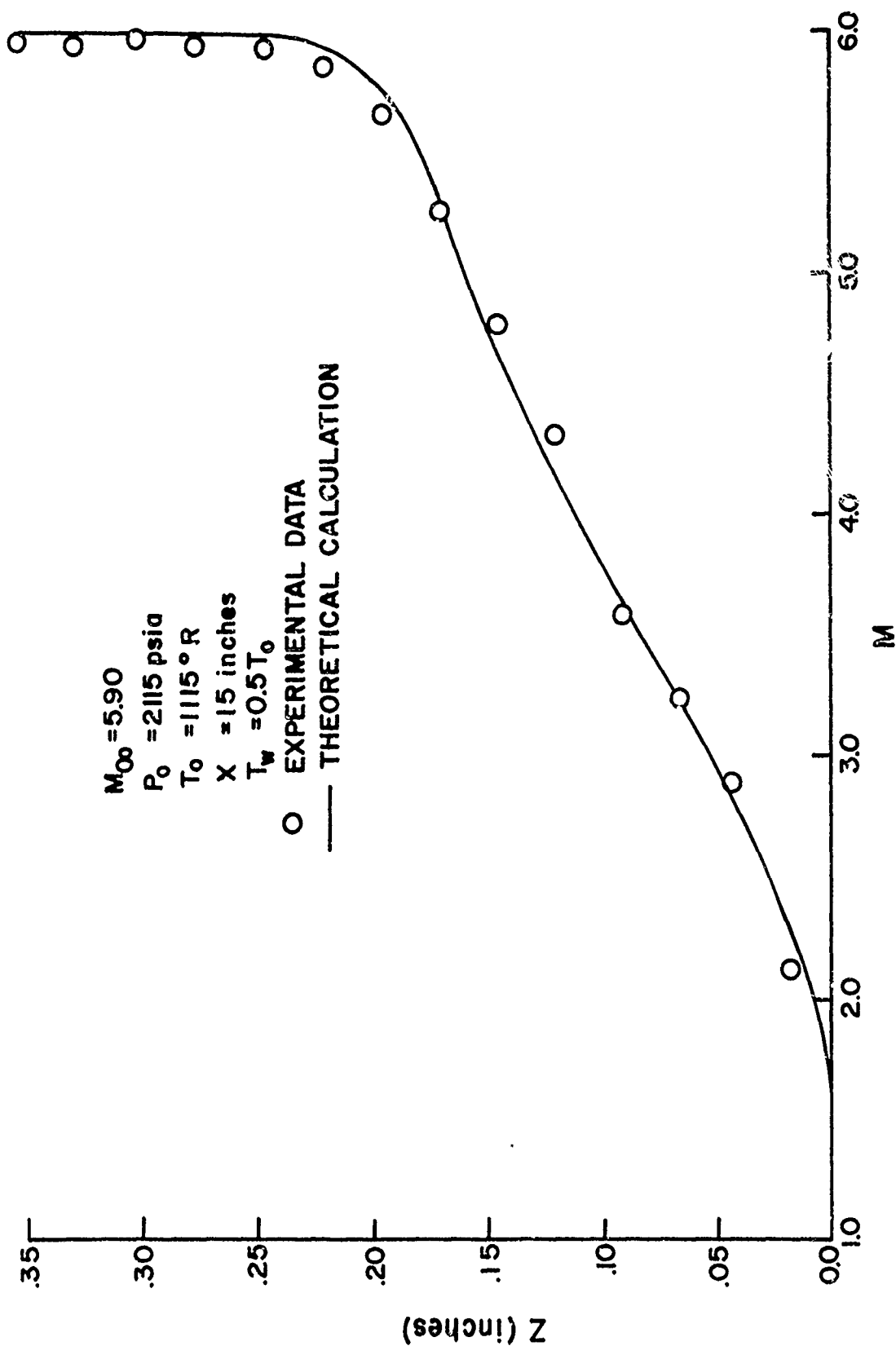


Figure 7. Mach Number Distribution Through Boundary Layer on Flat Plate at Station 5

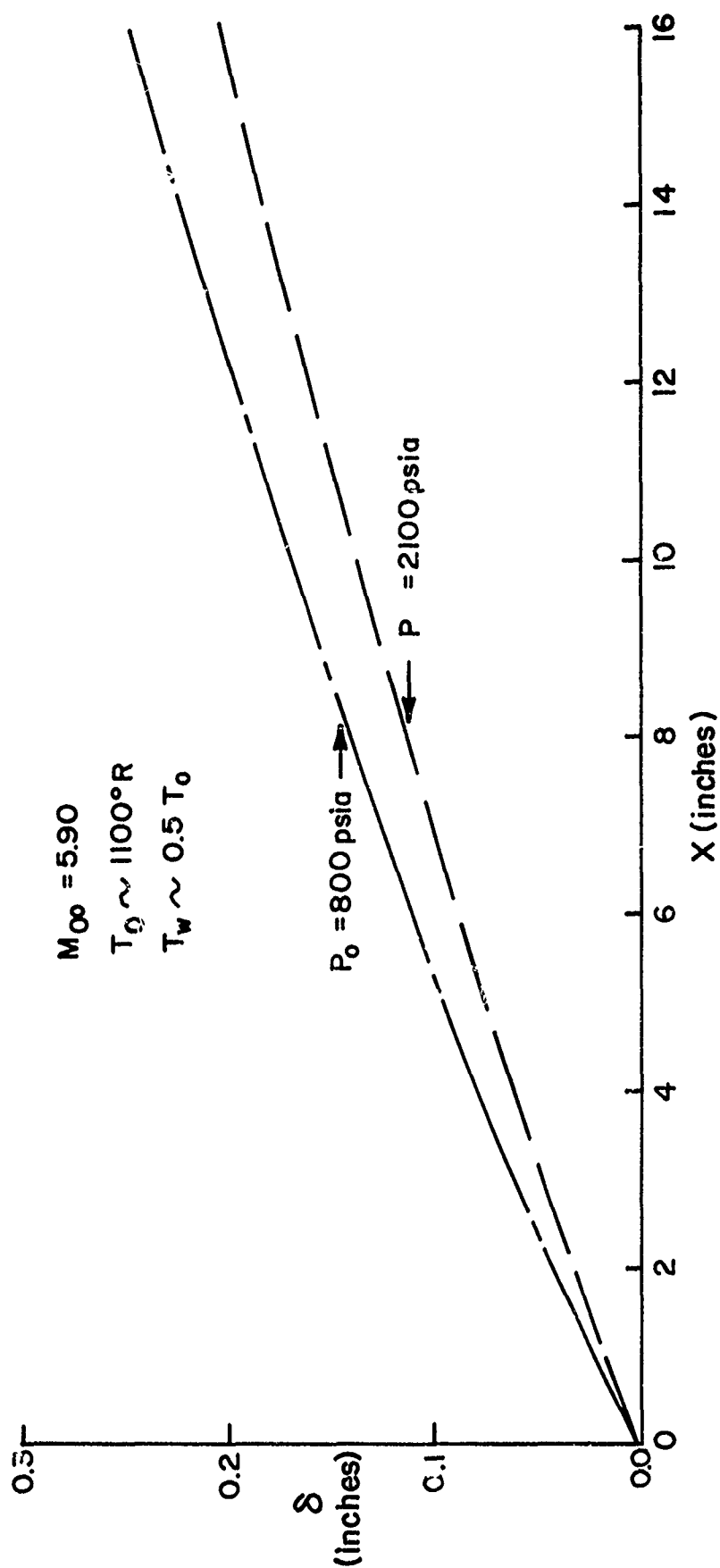


Figure 8. Boundary Layer Thickness Calculated from Finite Difference Scheme

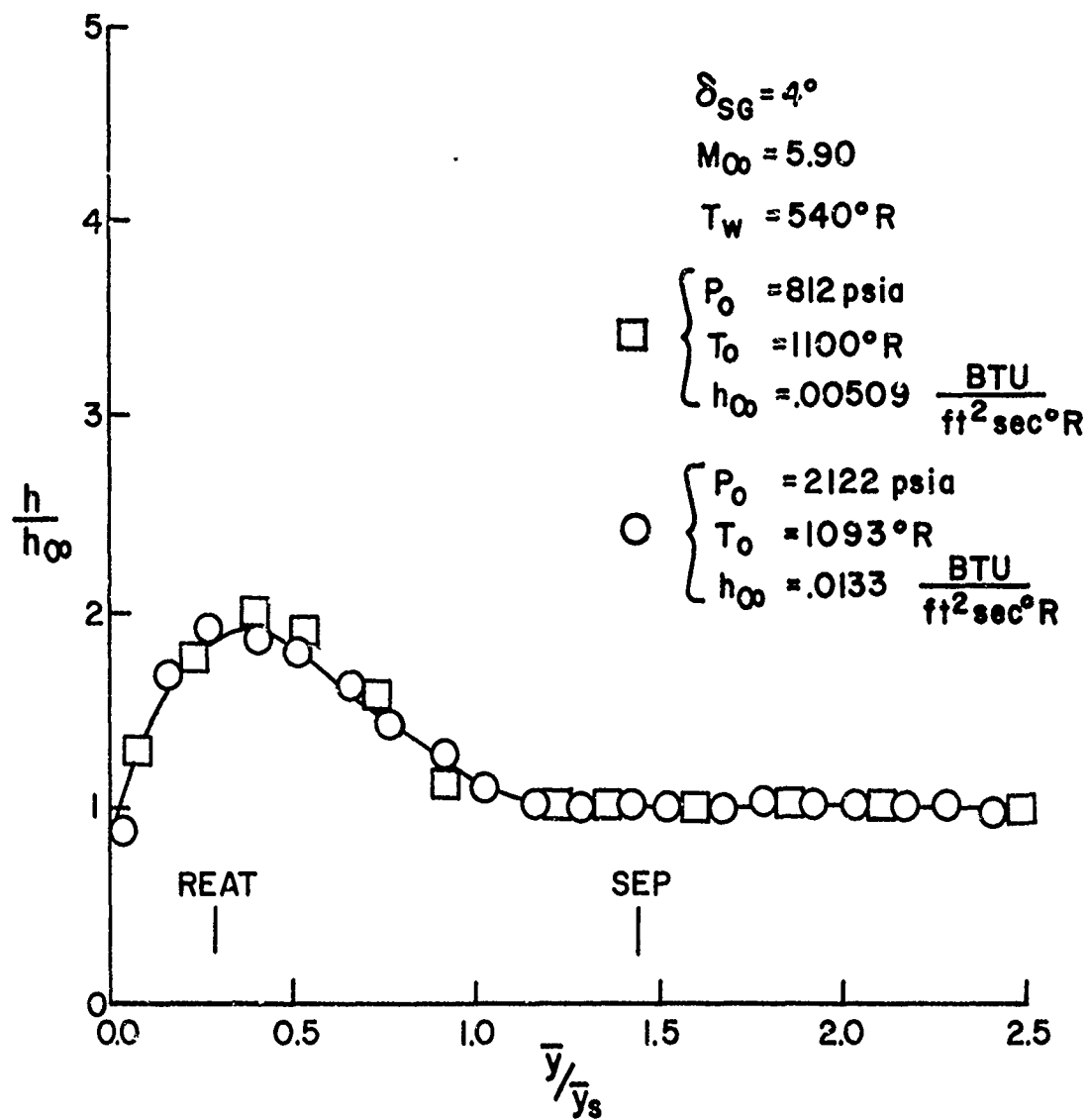


Figure 9a. Surface Heat Transfer Distributions for $Re = 1.0 \times 10^7$ and $3.0 \times 10^7 \text{ ft}^{-1}$ and $\delta_{SG} = 4^\circ$

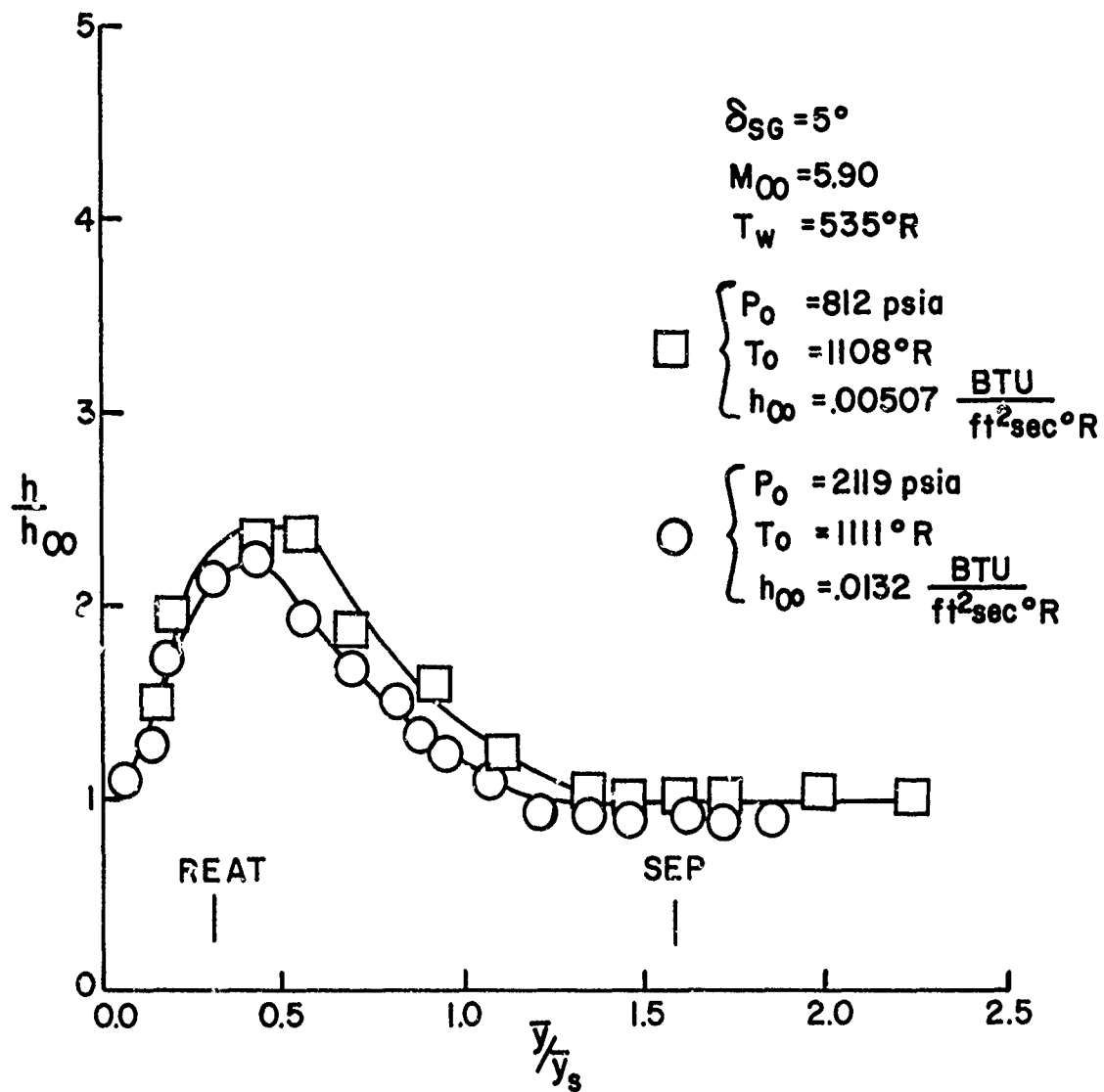


Figure 9b. Surface Heat Transfer Distributions for $Re = 1.0 \times 10^7$ and $3.0 \times 10^7 \text{ ft}^{-1}$ and $\delta_{SG} = 5^\circ$

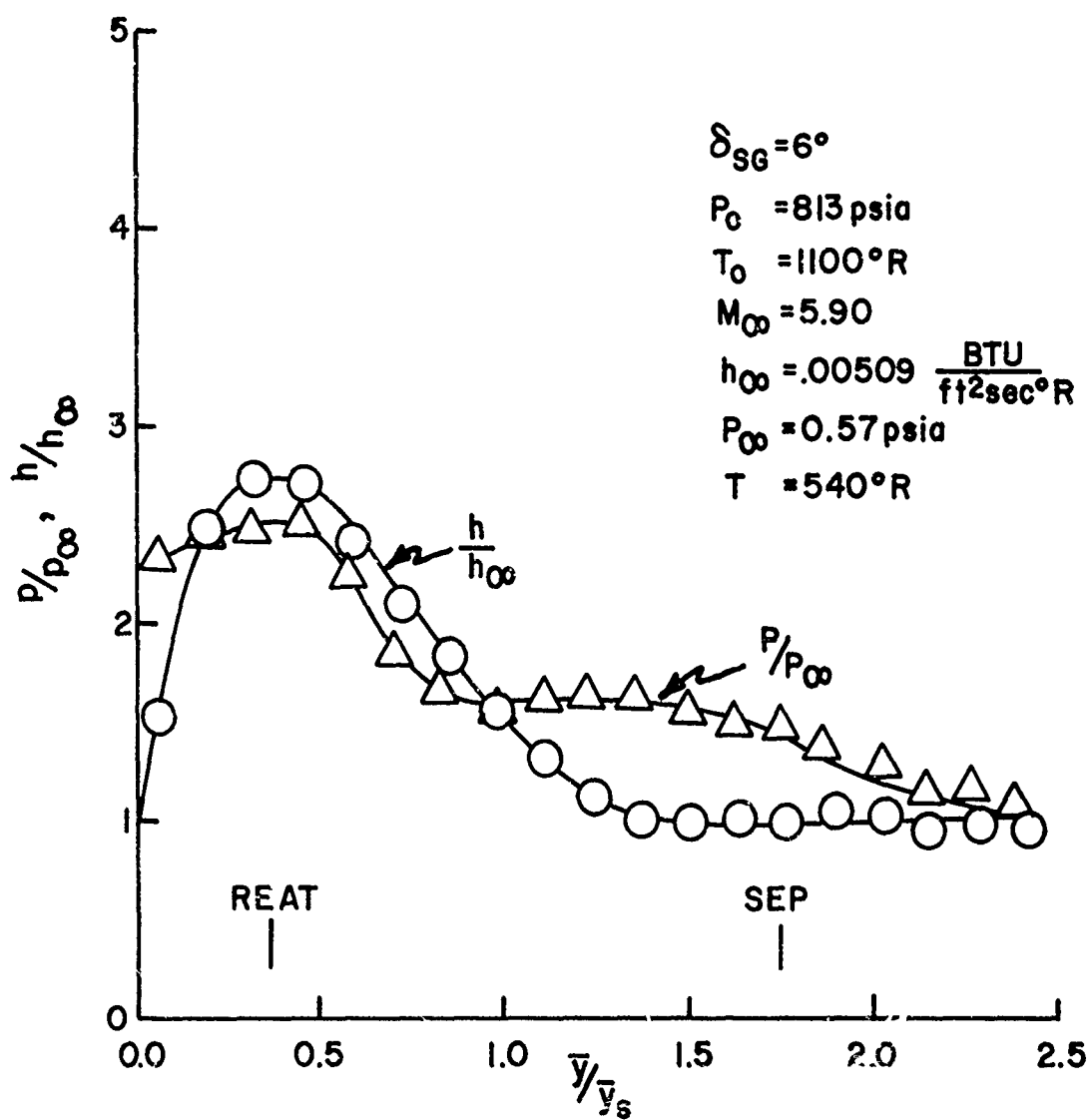


Figure 9c. Surface Pressure and Heat Transfer Distributions for $Re = 1.0 \times 10^7 \text{ ft}^{-1}$ and $\delta_{sg} = 6^\circ$

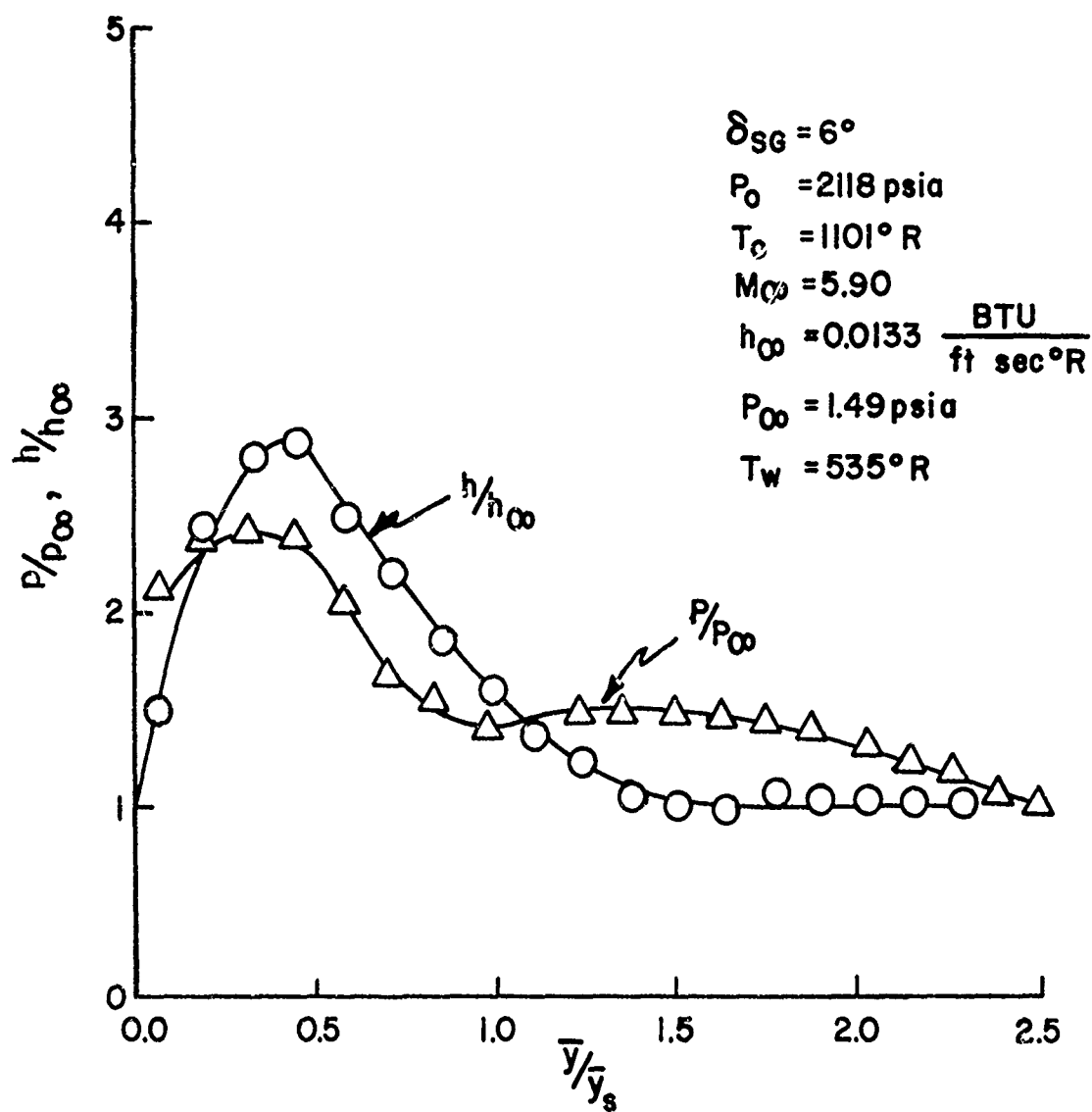


Figure 9d. Surface Pressure and Heat Transfer Distributions for $Re = 3.0 \times 10^7 \text{ ft}^{-1}$ and $\delta_{SG} = 6^\circ$

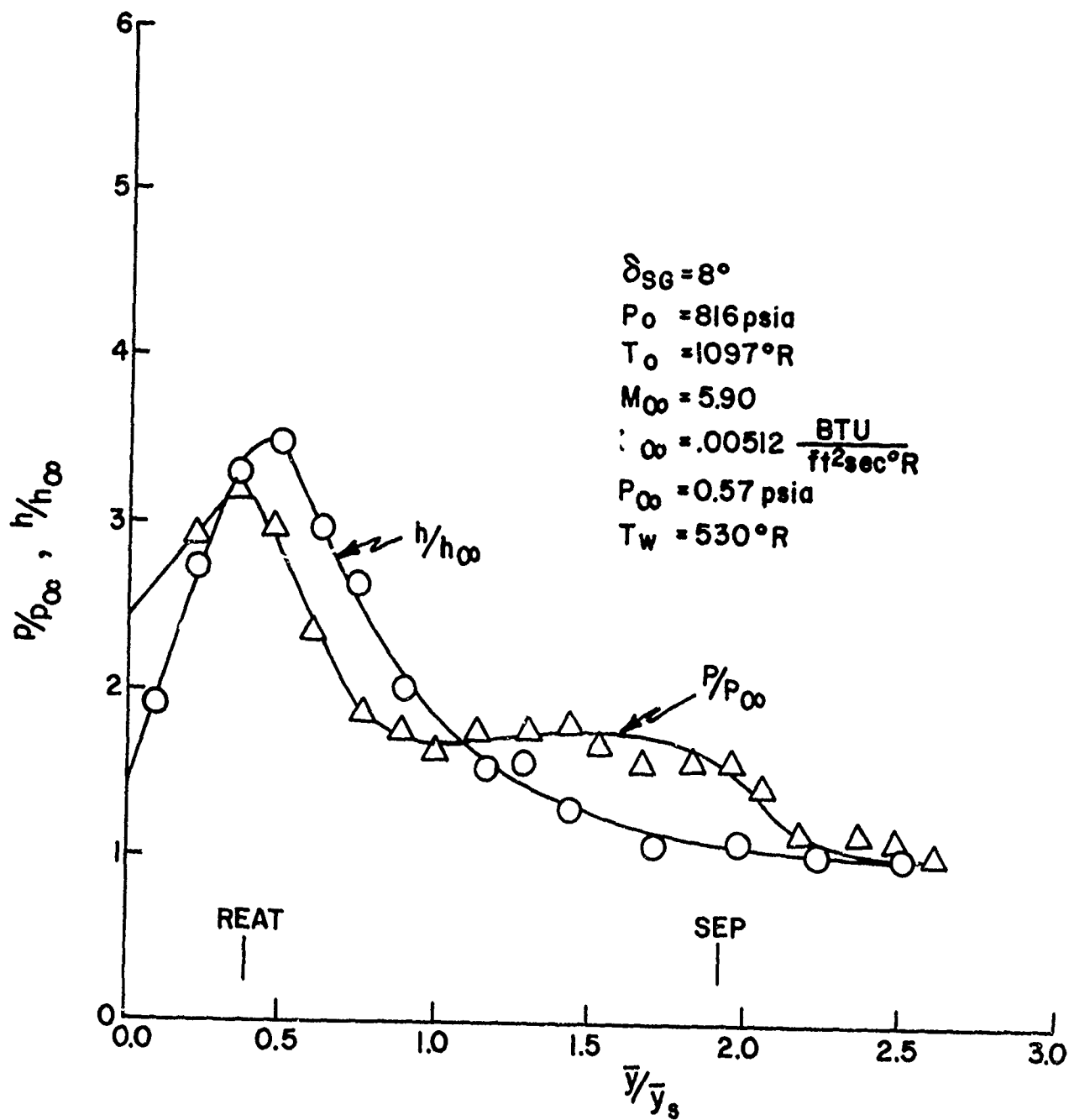


Figure 9e. Surface Pressure and Heat Transfer Distributions for $Re = 1.0 \times 10^7 \text{ ft}^{-1}$ and $\delta_{SG} = 8^\circ$

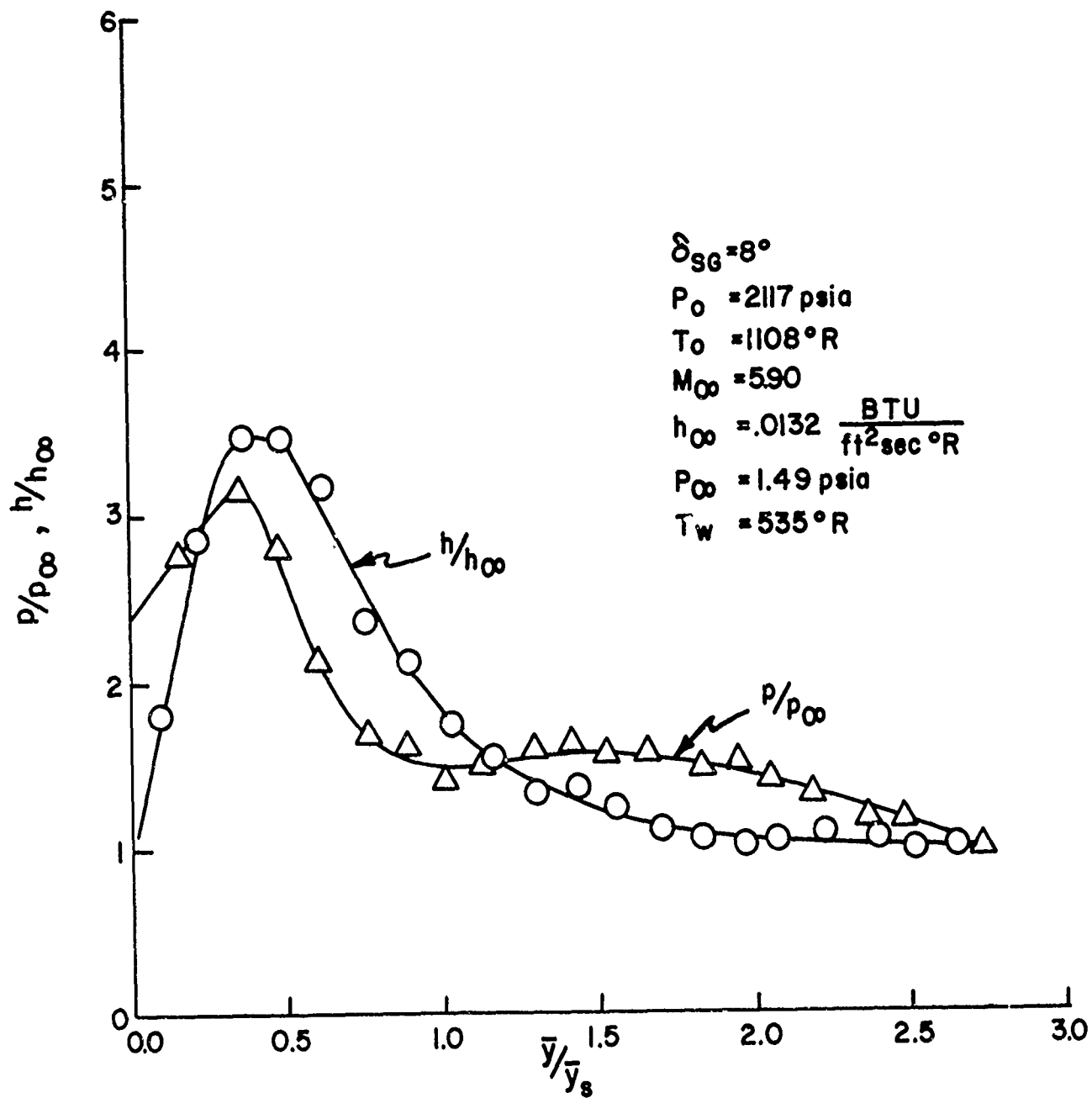


Figure 9f. Surface Pressure and Heat Transfer Distributions for $Re = 3.0 \times 10^7 \text{ ft}^{-1}$ and $\delta_{SG} = 8^\circ$

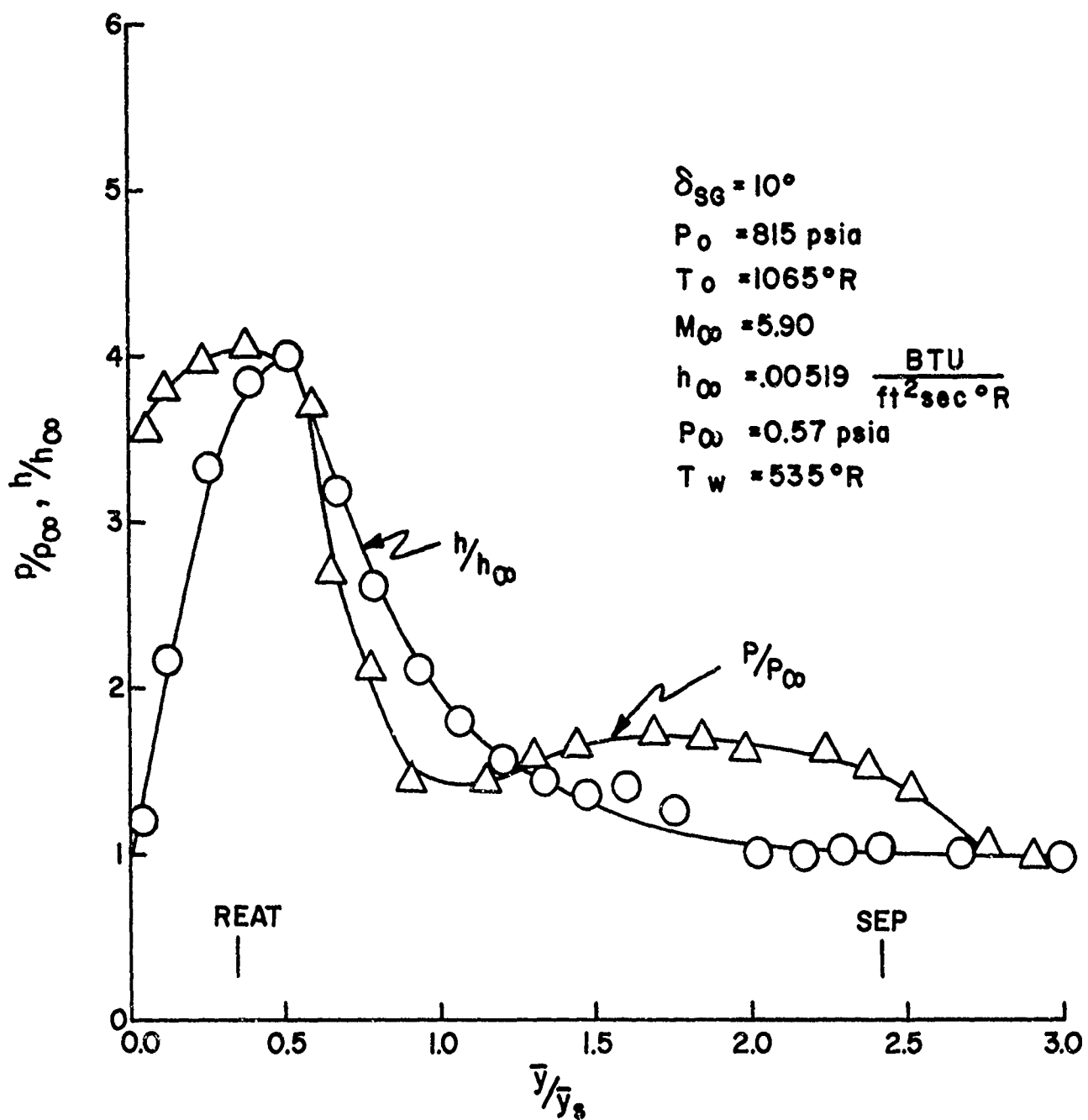


Figure 9g. Surface Pressure and Heat Transfer Distributions for $Re = 1.0 \times 10^7 \text{ ft}^{-1}$ and $\delta_{SG} = 10^\circ$

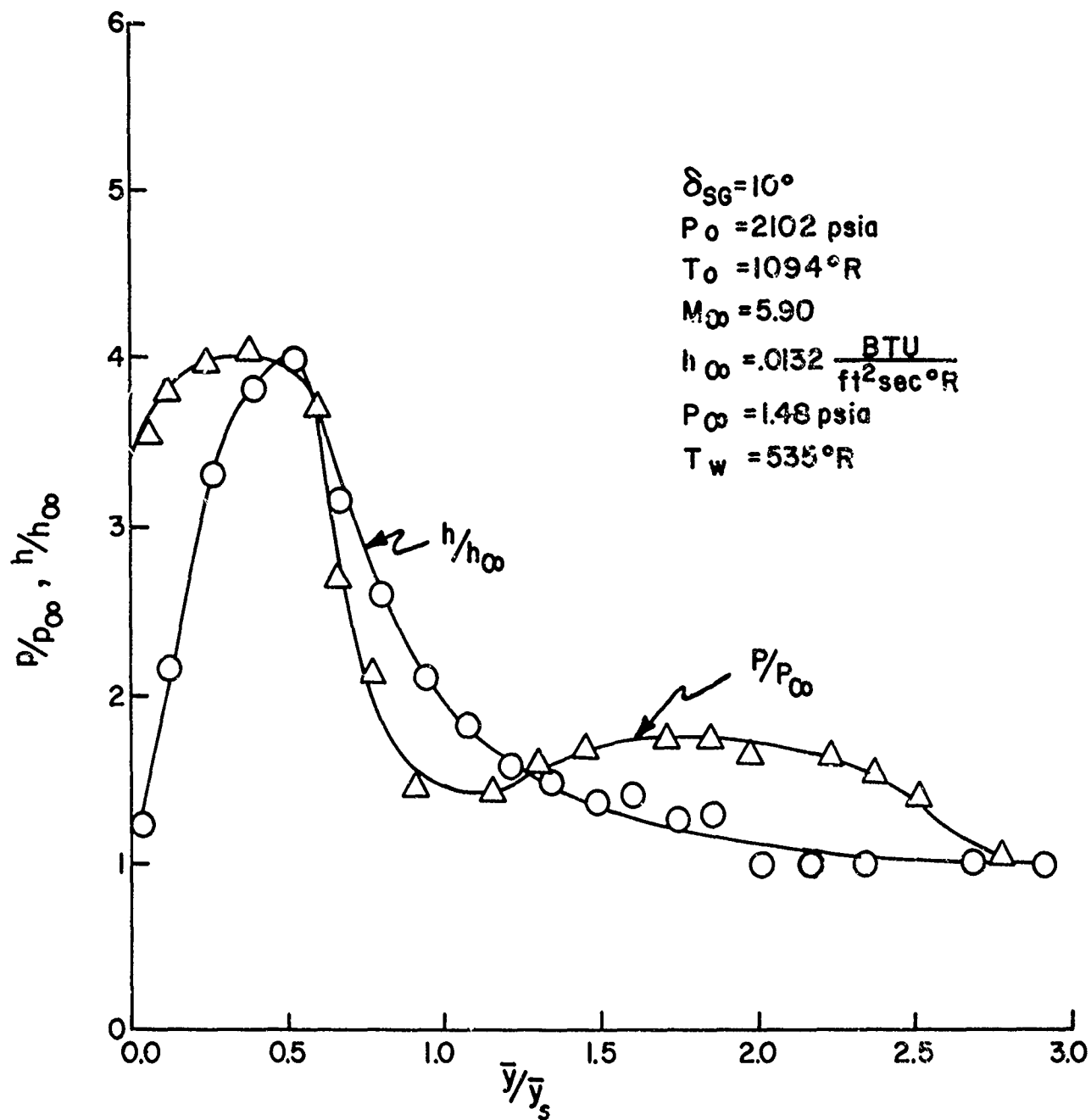


Figure 9h. Surface Pressure and Heat Transfer Distributions for $Re = 3.0 \times 10^7 \text{ ft}^{-1}$ and $\delta_{SG} = 10^\circ$

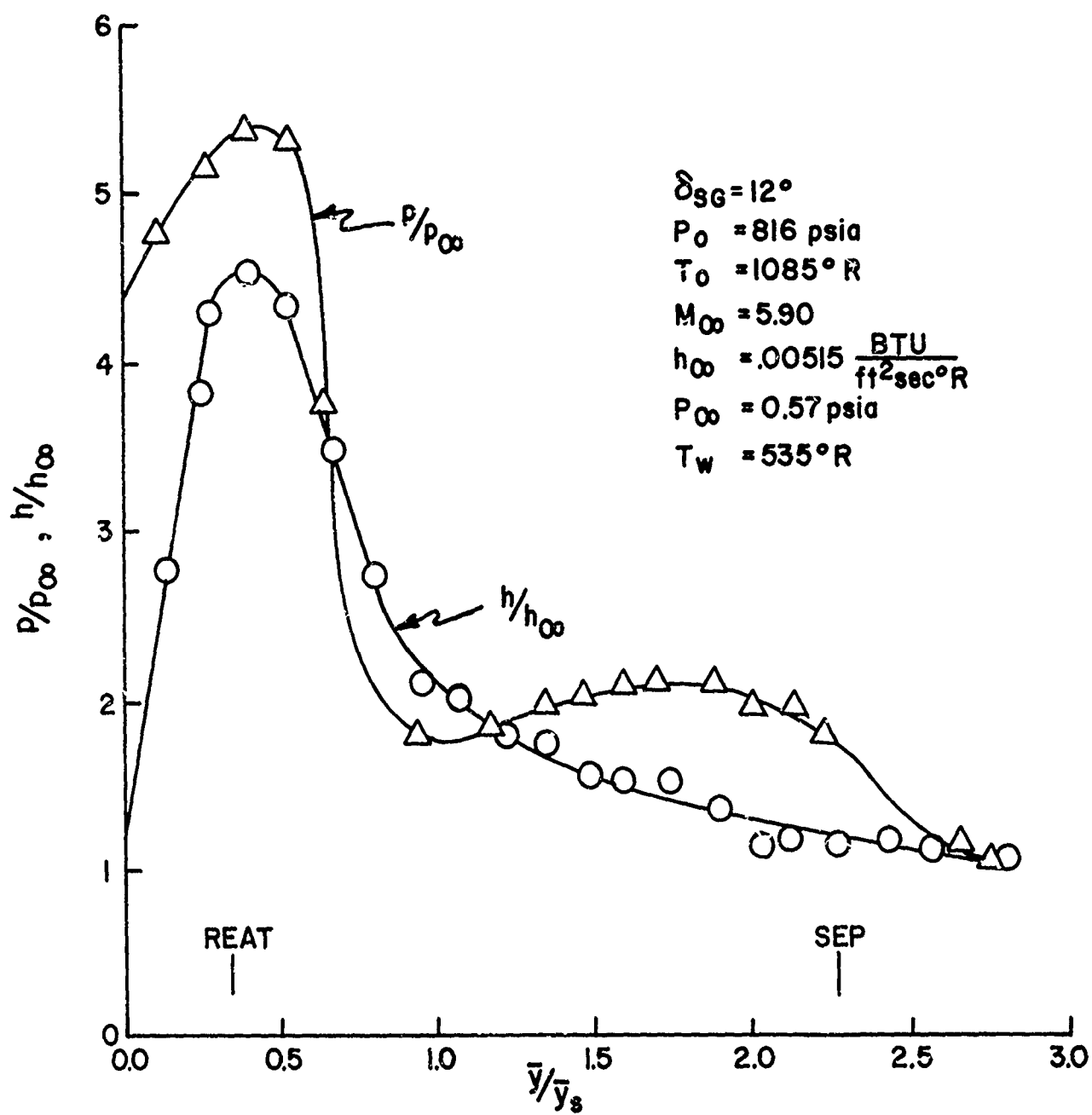


Figure 9i. Surface Pressure and Heat Transfer Distributions for $Re = 1.0 \times 10^7 \text{ ft}^{-1}$ and $\delta_{SG} = 12^\circ$

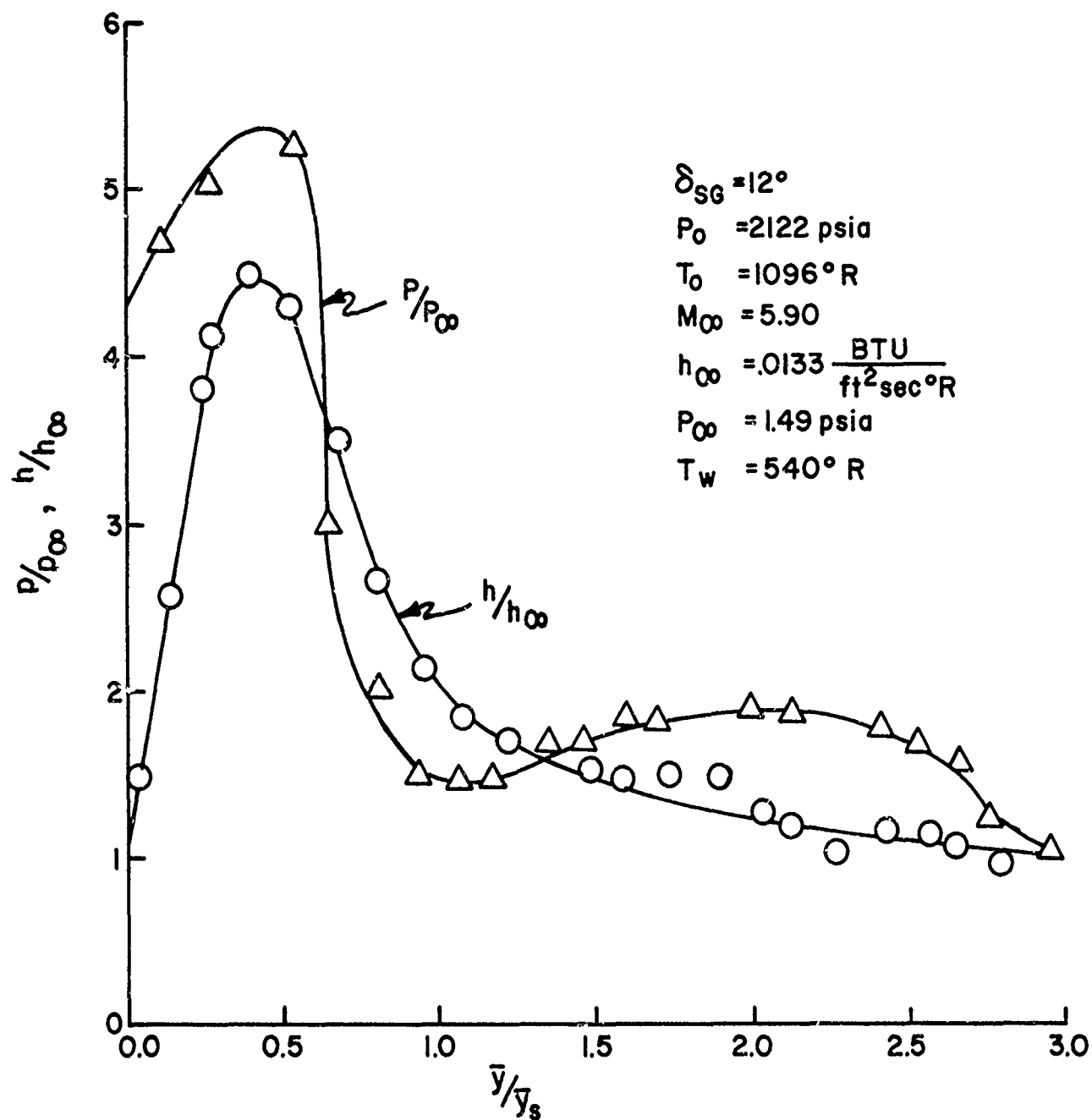


Figure 9j. Surface Pressure and Heat Transfer Distributions for $Re = 3.0 \times 10^7 \text{ ft}^{-1}$ and $\delta_{SG} = 12^\circ$

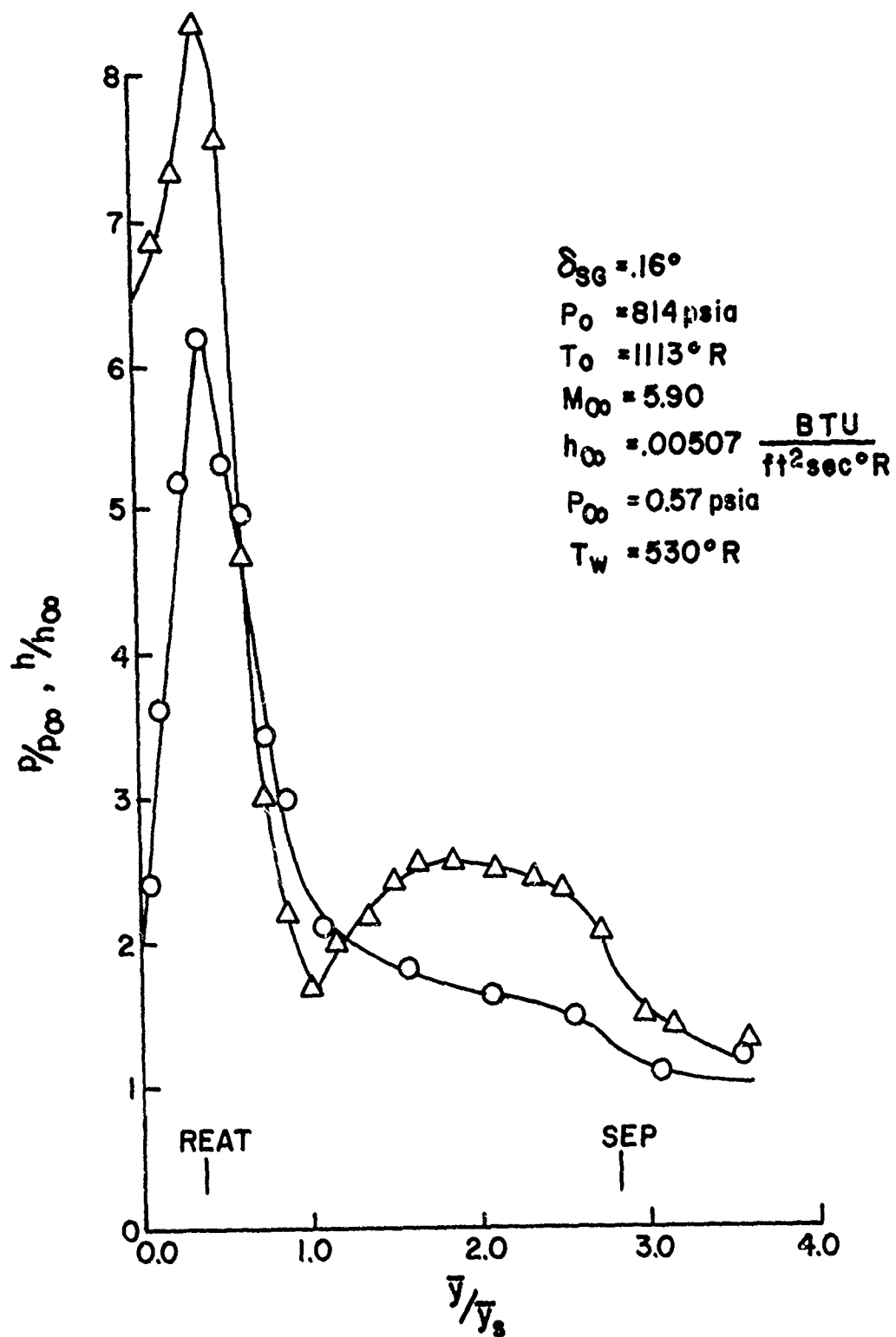


Figure 9k. Surface Pressure and Heat Transfer Distributions for $Re = 1.0 \times 10^7 \text{ ft}^{-1}$ and $\delta_{SG} = 16^\circ$

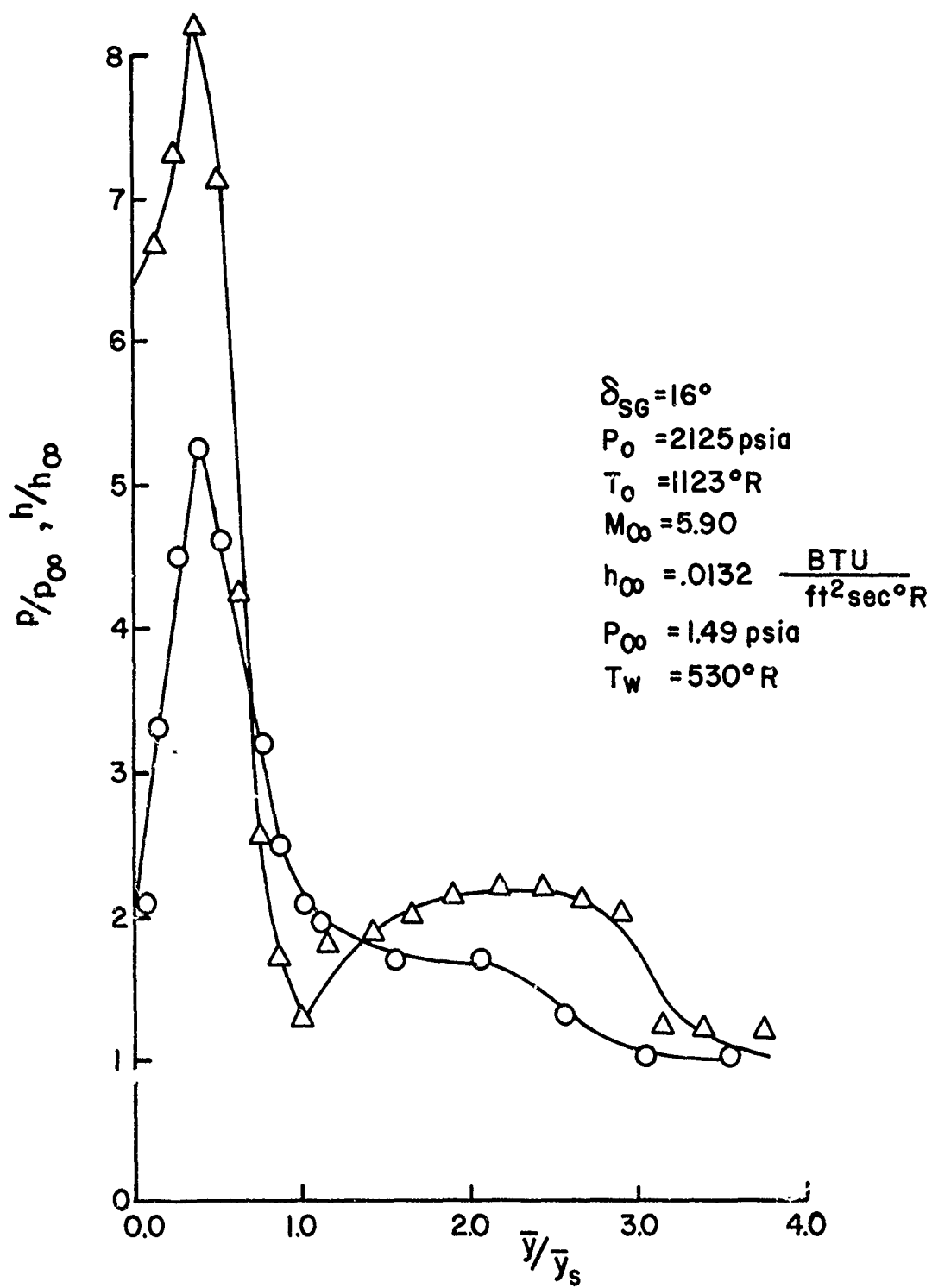


Figure 91. Surface Pressure and Heat Transfer Distributions for $Re = 3.0 \times 10^7 \text{ ft}^{-1}$ and $\delta_{SG} = 16^\circ$

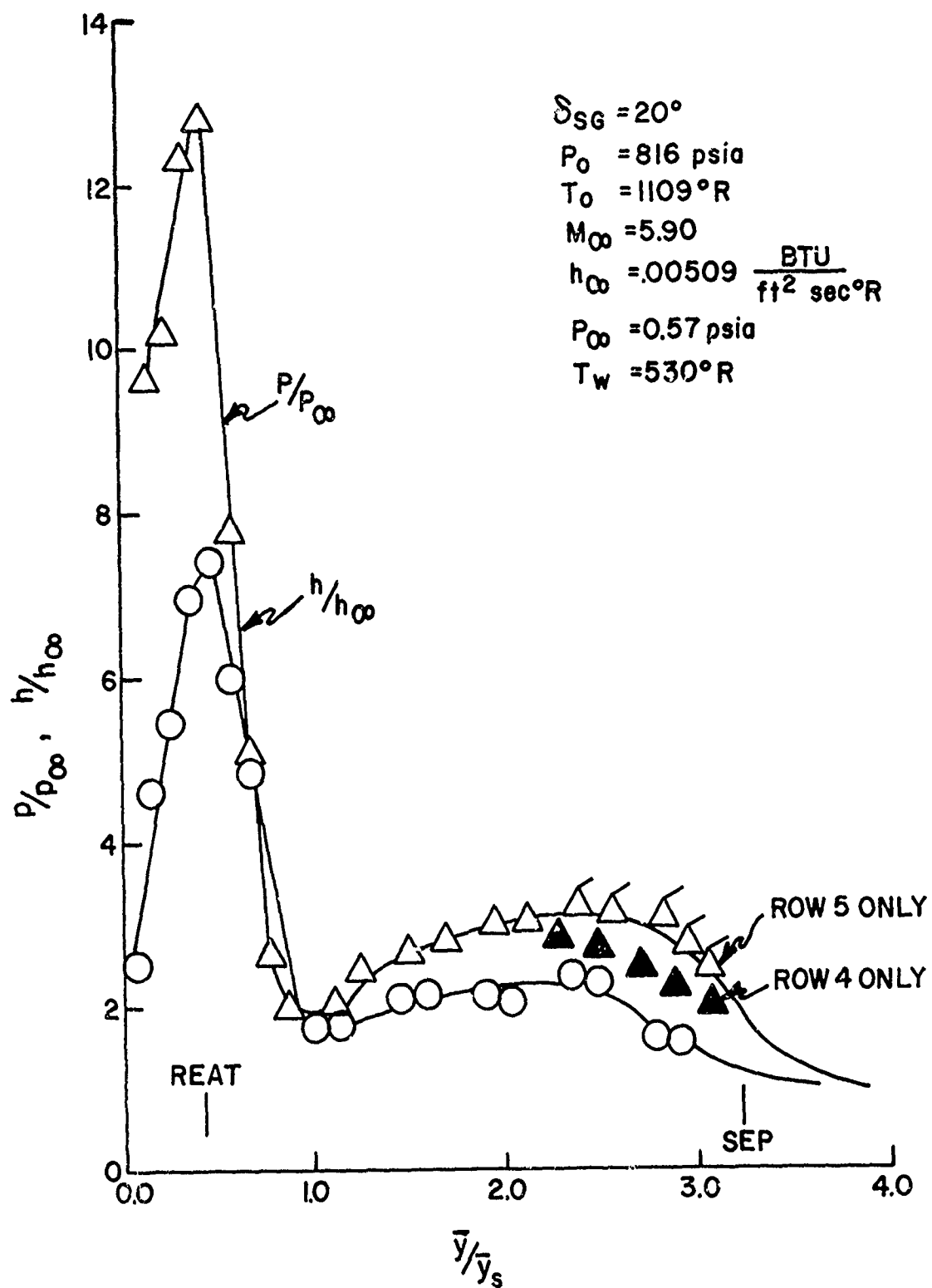


Figure 9m. Surface Pressure and Heat Transfer Distributions for $Re = 1.0 \times 10^7 \text{ ft}^{-1}$ and $\delta_{SG} = 20^\circ$

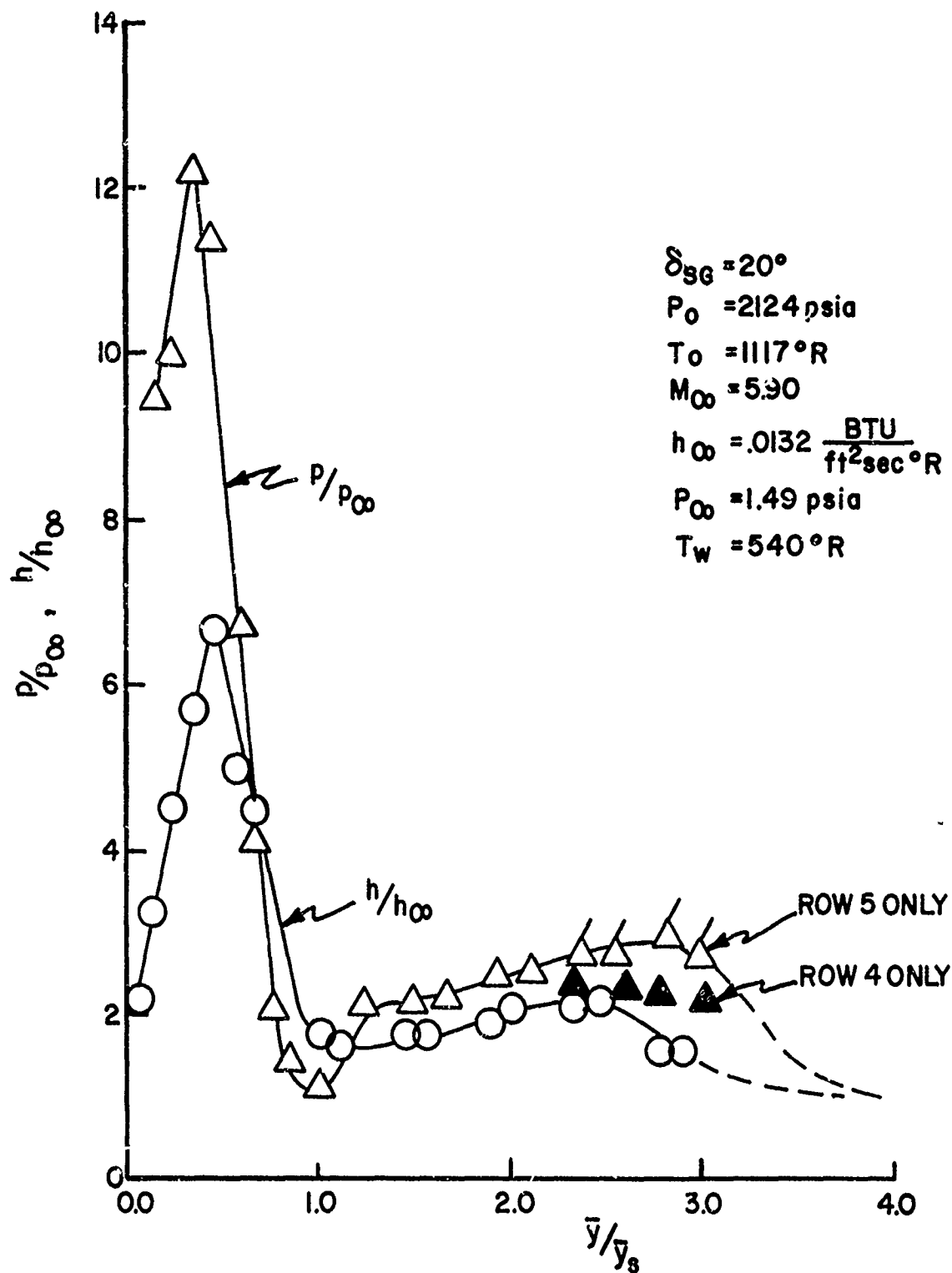


Figure 9n. Surface Pressure and Heat Transfer Distributions for $Re = 3.0 \times 10^7 \text{ ft}^{-1}$ and $\delta_{SG} = 20^\circ$

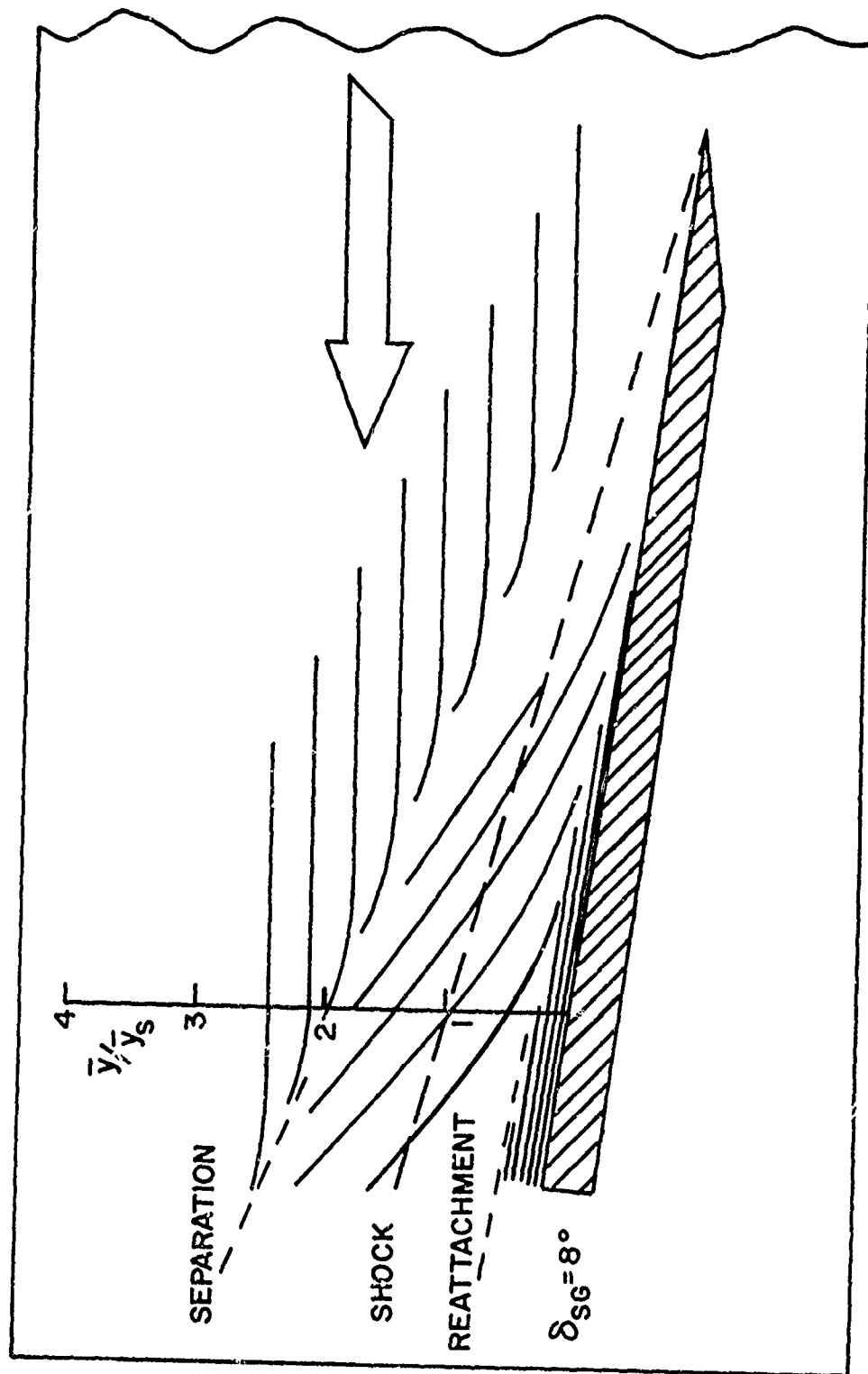


Figure 10a. Sketch of Oil Flow Photograph for $Re \approx 1.0 \times 10^7 \text{ ft}^{-1}$ and $\delta_{SG} = 8^\circ$

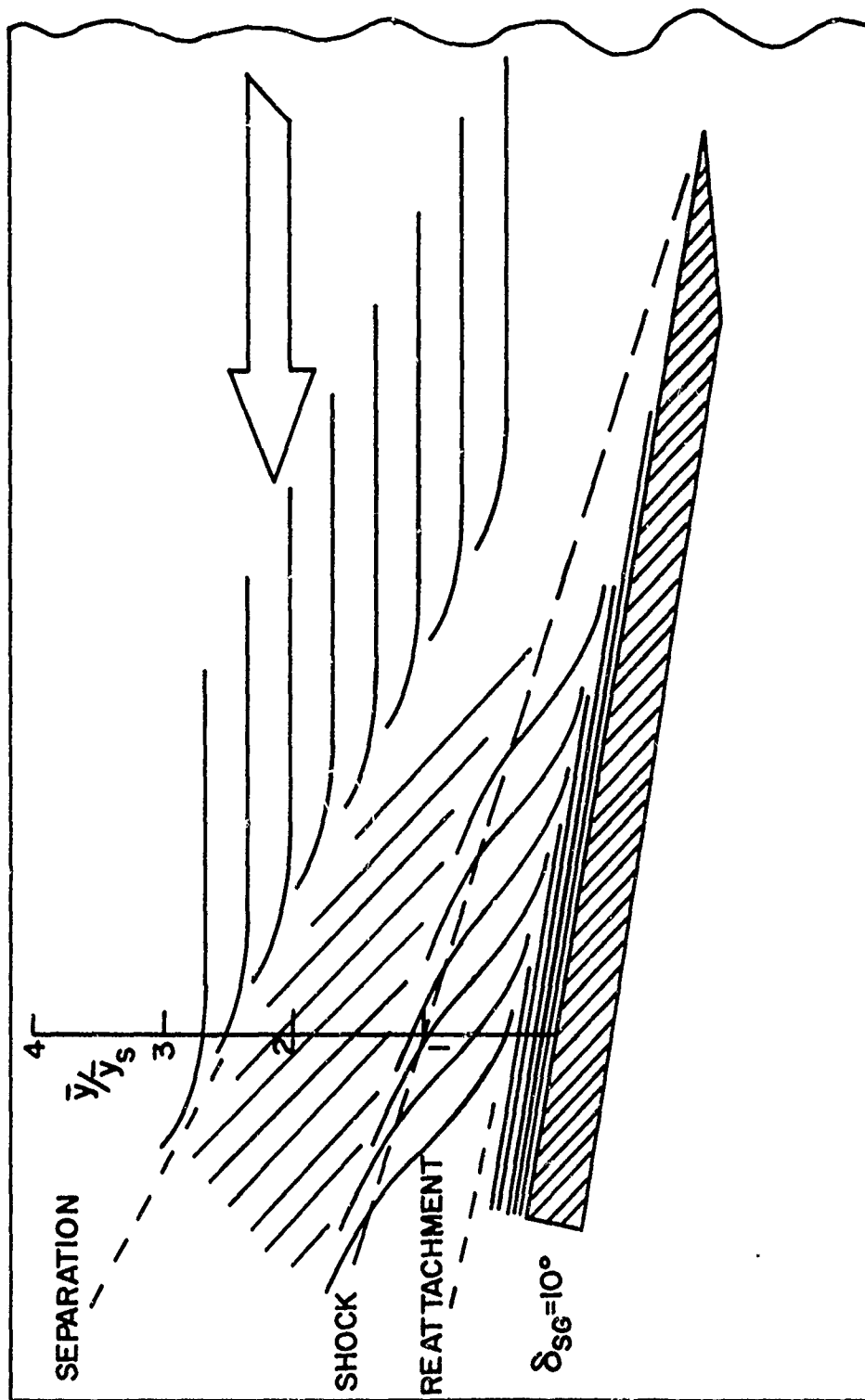


Figure 10b. Sketch of Oil Flow Photograph for $Re = 1.0 \times 10^7 \text{ ft}^{-1}$
and $\delta_{SG} = 10^\circ$

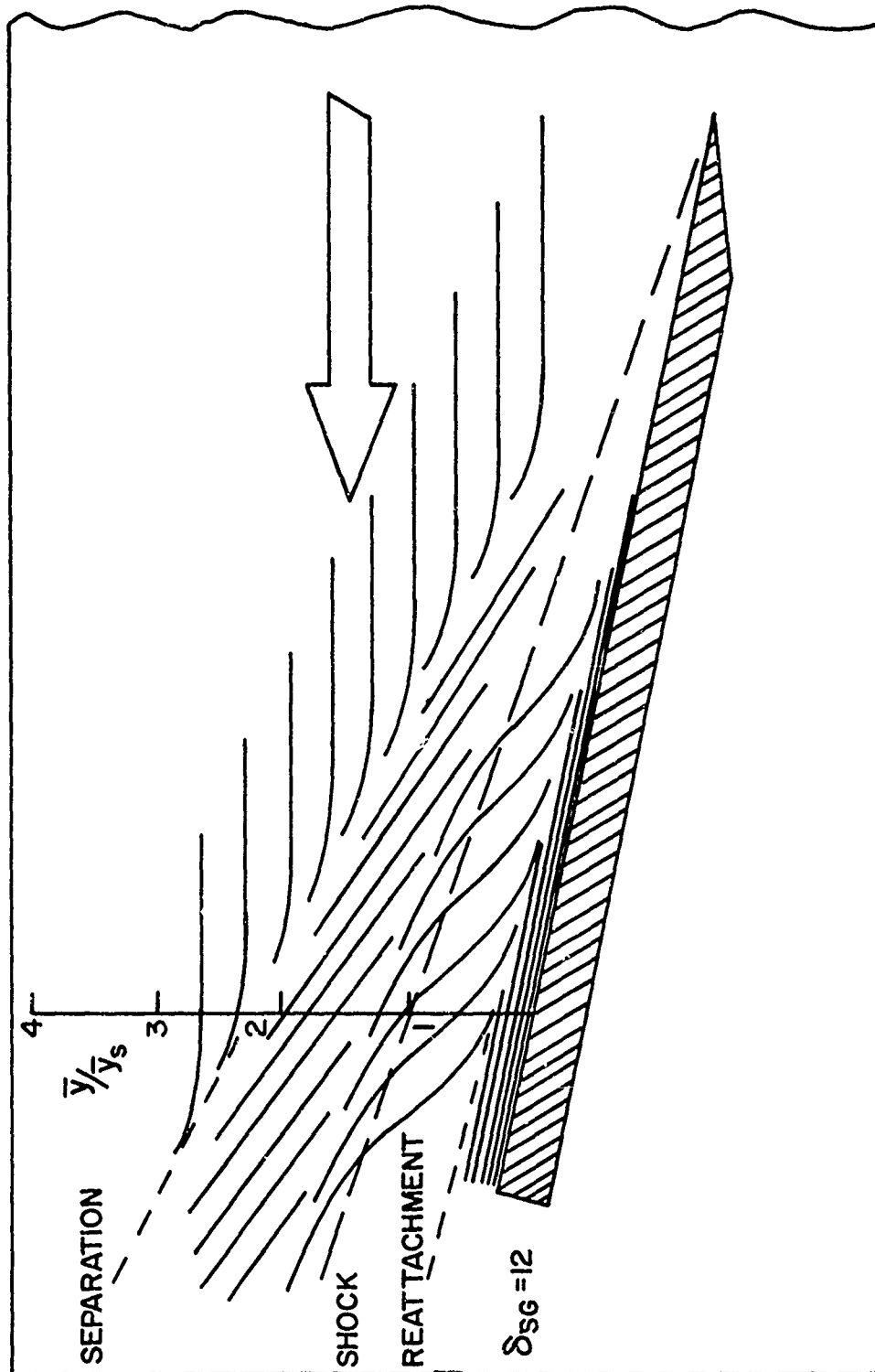


Figure 10c. Sketch of Oil Flow Photograph for $Re = 1.0 \times 10^7 \text{ ft}^{-1}$ and $\delta_{SG} = 12^\circ$

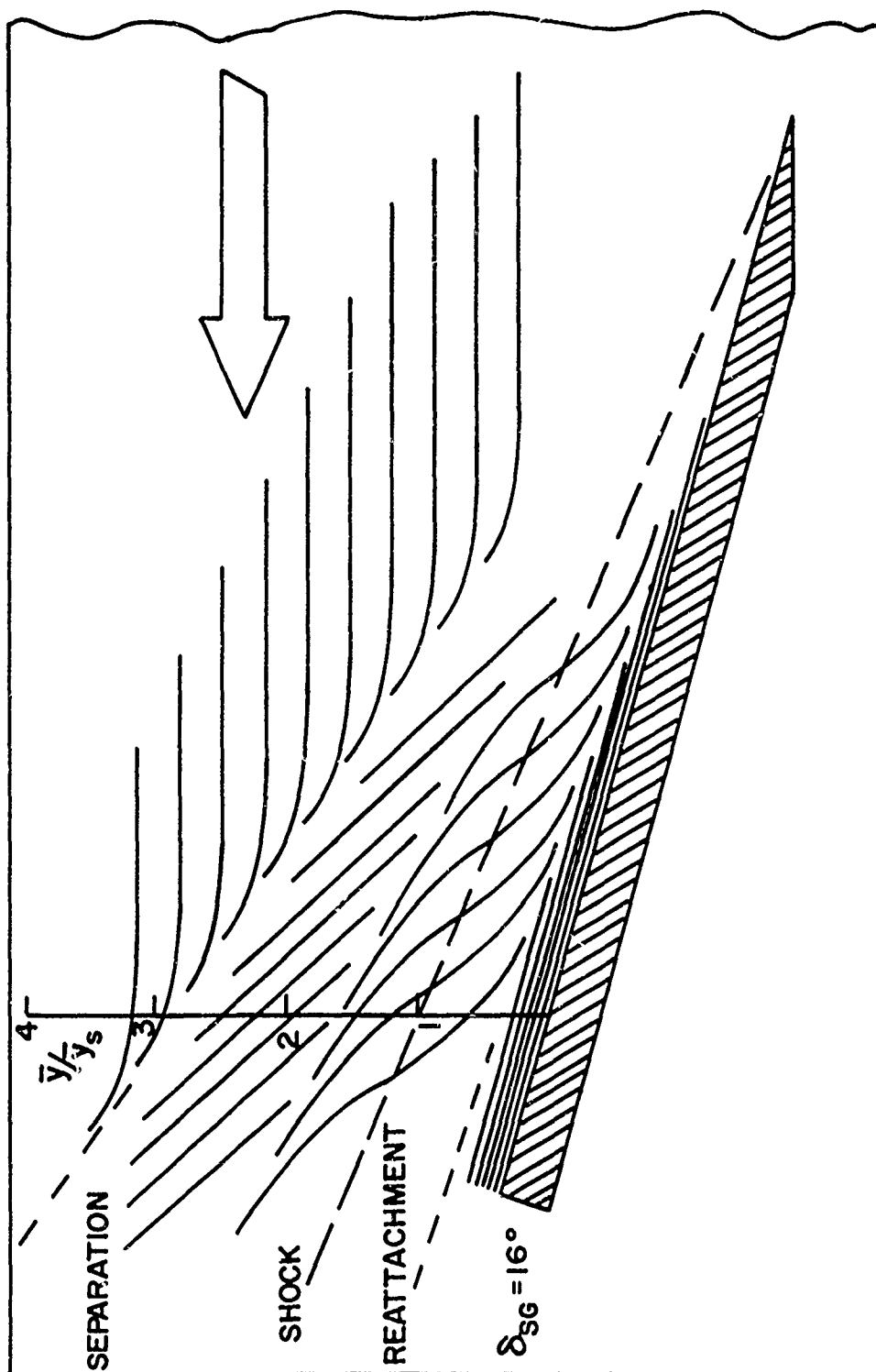


Figure 10d. Sketch of Oil Flow Photograph for $Re = 1.0 \times 10^7 \text{ ft}^{-1}$ and $\delta_{SG} = 16^\circ$

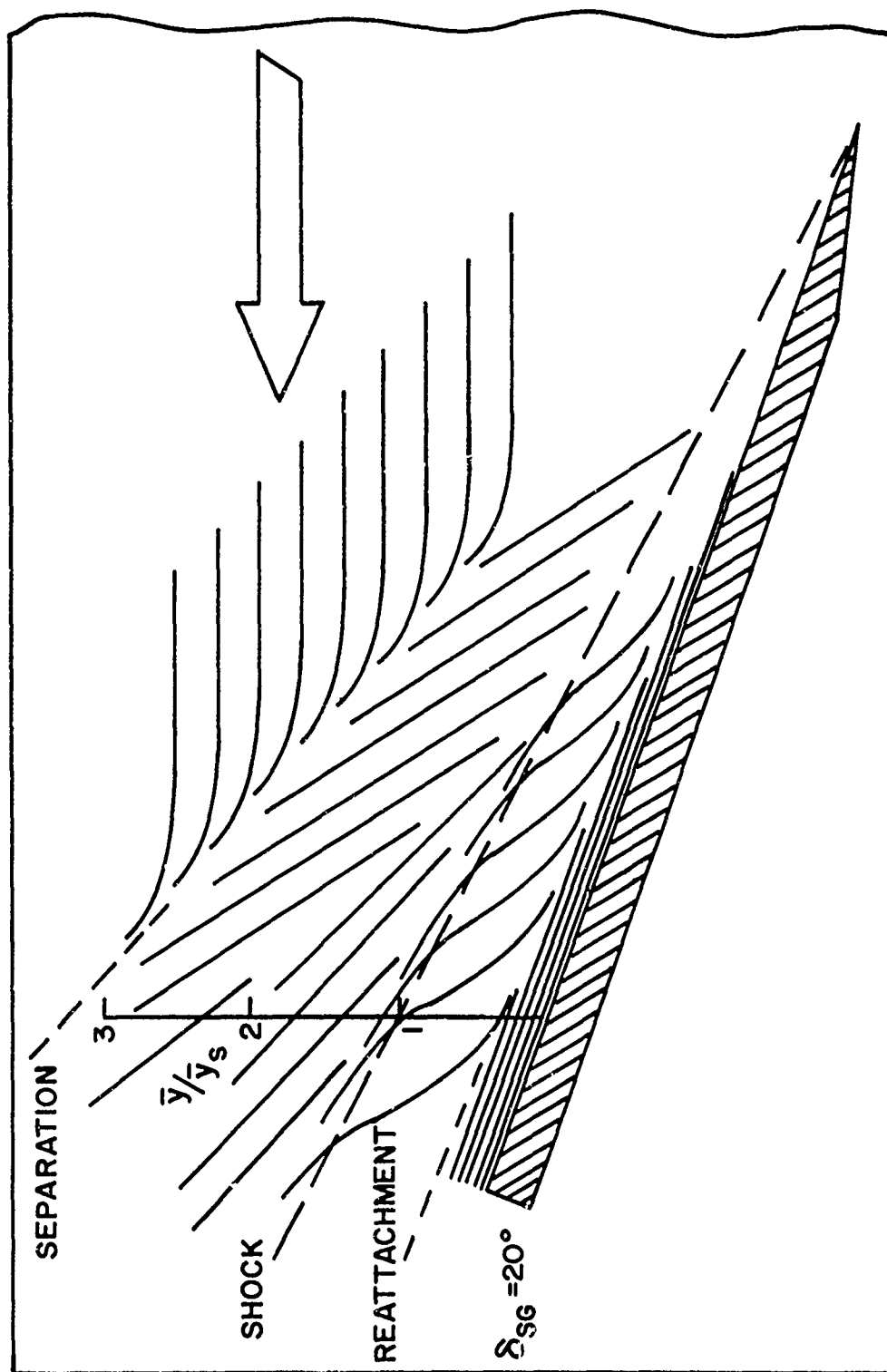


Figure 10e. Sketch of Oil Flow Photograph for $Re = 1.0 \times 10^7 \text{ ft}^{-1}$
and $\delta_{SG} = 20^\circ$

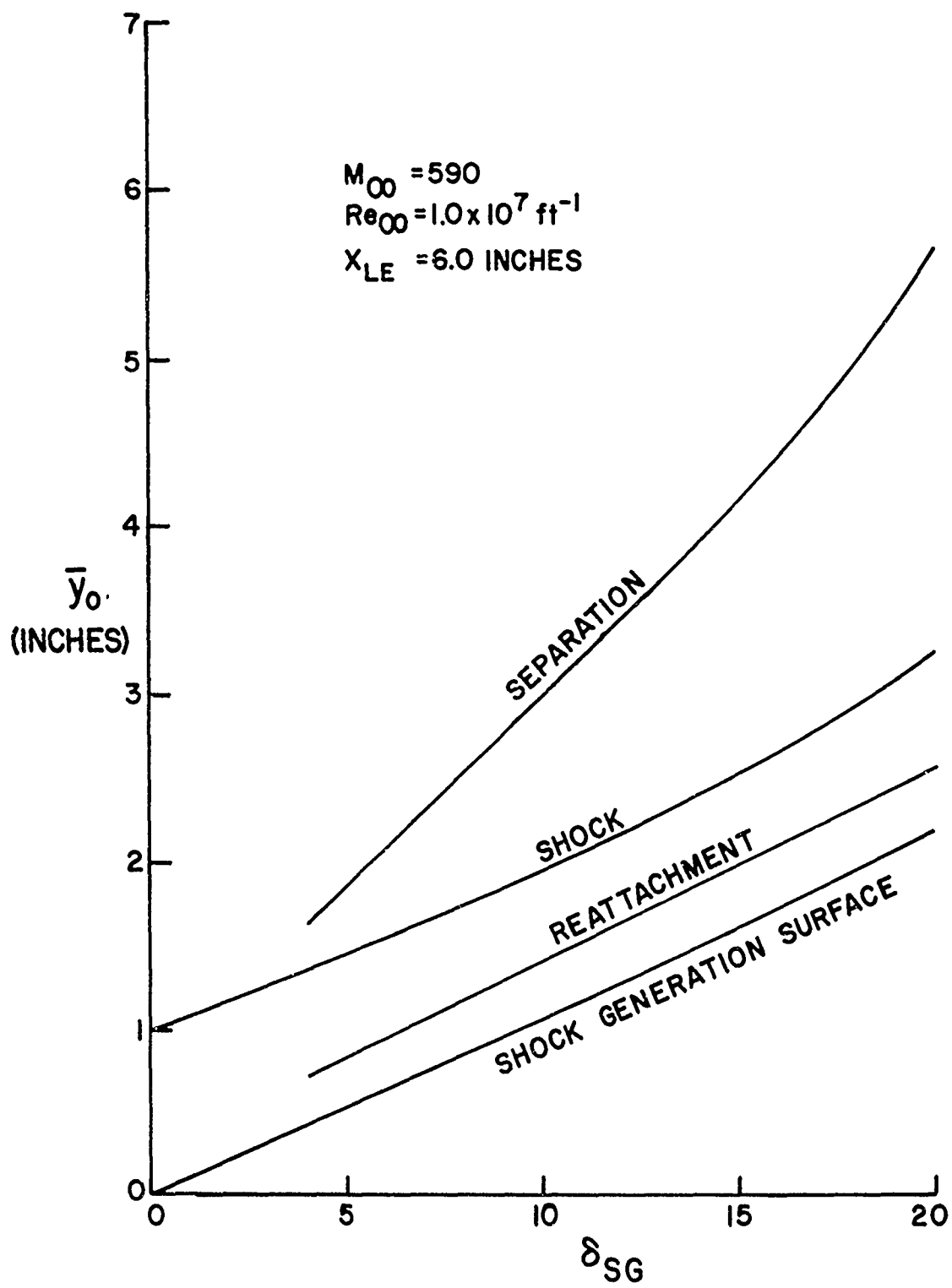


Figure 11. Lateral Distance to Shock Generator Surface, Shock, Reattachment Line and Separation Line Versus Shock Generator Angle

REFERENCES

1. Fiore, A. W. and Law, C. H., "Aerodynamic Calibration of the Aerospace Research Laboratories' Mach 6 High Reynolds Number Facility," ARL 75-0028, Aerospace Research Laboratories, Wright-Patterson Air Force Base, Ohio, January 1975.
2. Christophel, R. G. and Rockwell, W. A., "Tabulated Mach-6 3-D Shock Wave-Turbulent Boundary Layer Interaction Heat Transfer Data," AFFDL-TM-74-212-FXG, Air Force Flight Dynamics Laboratory, Wright-Patterson Air Force Base, Ohio, November 1974.

LIST OF SYMBOLS

h	Heat transfer coefficient, $\text{BTU}/\text{ft}^2 \text{ sec}^\circ\text{R}$
h_∞	Local undisturbed heat transfer coefficient
M	Mach number
P	Pressure
Re	Reynolds number
T	Temperature
X	Axial distance from flat plate leading edge
X_{LE}	Axial distance from shock generator leading edge
Y	Lateral distance from flat plate edge
\bar{Y}	Lateral distance from shock generator surface
\bar{Y}_S	Lateral distance from shock generator surface to shock wave
\bar{Y}_O	Lateral distance from shock generator surface with shock generator at zero degrees
Z	Vertical distance from flat plate surface
δ	Boundary layer thickness
δ_{SG}	Shock generator angle

SUBSCRIPTS

∞	Freestream condition
o	Stagnation condition
w	Wall condition